

Research Article

Consensus of Multi-Integral Fractional-Order Multiagent Systems with Nonuniform Time-Delays

Jun Liu ^{1,2}, Wei Chen ¹, Kaiyu Qin ², and Ping Li ¹

¹School of Control Engineering, Chengdu University of Information Technology, Chengdu 610225, China

²School of Aeronautics and Astronautics, University of Electronic Science and Technology of China, Chengdu 611731, China

Correspondence should be addressed to Jun Liu; liujun@cuit.edu.cn

Received 2 June 2018; Revised 15 August 2018; Accepted 17 October 2018; Published 1 November 2018

Guest Editor: Christos K. Volos

Copyright © 2018 Jun Liu et al. This is an open access article distributed under the Creative Commons Attribution License, which permits unrestricted use, distribution, and reproduction in any medium, provided the original work is properly cited.

Consensus of fractional-order multiagent systems (FOMASs) with single integral has been widely studied. However, the dynamics with multiple integral (especially double integral to sextuple integral) also exist in FOMASs, and they are rarely studied at present. In this paper, consensus problems for multi-integral fractional-order multiagent systems (MIFOMASs) with nonuniform time-delays are addressed. The consensus conditions for MIFOMASs are obtained by a novel frequency-domain method which properly eliminates consensus problems of the systems associated with nonuniform time-delays. Besides, the method revealed in this paper is applicable to classical high-order multiagent systems which is a special case of MIFOMASs. Finally, several numerical simulations with different parameters are performed to validate the correctness of the results.

1. Introduction

The research related to multiagent systems (MASs) has been going on for decades, due to its many meaningful applications, e.g., sweep coverage control of MASs [1], flocking behavior of mobile robots [2], and coordinated attitude control of a formation of satellites [3]. Consensus is an agreement on the quality of certain concerns about the specific states of all agents, which is one of the most fundamental requirements for the research on MASs.

Up to now, numerous studies have been conducted to resolve the problems about consensus of MASs with different dynamics. During the past decades, a lot of results have been accomplished about consensus of first-order MASs [4–11]. In [4], a simple model was presented for the phase transition of a set of self-driven particle, and it was demonstrated that the headings of all agents in MASs converged to a common value by simulation. In [5], authors provided some theoretical explanations for Vicsek's linearized model and analyzed the alignment of undirected switching topologies of agents that were regularly connected. Based on the research works of [5], more relaxed consensus conditions over dynamic

switching topologies were given in [6, 7]. Authors in [8] put forward a framework about consensus theory of MASs with directed information flow, link/node failures, time-delays, and so on. Robust H_∞ control about consensus problems for MASs with parameter uncertainties, external disturbances, nonidentical state, and time-delays was discussed in [9]. In recent years, more and more researchers have paid more attention to consensus of second-order MASs [12–16]. For instance, authors in [12] investigated consensus problems for second-order continuous-time MASs in the presence of jointly connected topologies and time-delay. In [13], two types of consensus problems for second-order MASs with and without delay over switching topology and directed topology were studied. In [14], the local consensus problem for second-order MASs whose dynamics were nonlinear dynamics under directed and switching random topology was discussed, and several sufficient conditions were derived to ensure the MASs reach consensus. Furthermore, taking into account the fact that high-order MASs were widely used, consensus problems for high-order MASs have been studied in [17–21]. In particular, the output consensus problem in [17] was addressed for high-order MASs with external disturbances,

and some conditions were derived to ensure consensus for the MASs. The consensus problems in [18] were considered for a class of high-order MASs with time-delays and switching networks, and a nearest-neighbour rule was designed and some conditions were derived to guarantee consensus for the systems with time-delays. The conditions of consensus in [21] for high-order MASs with nonuniform time-delays were proposed by a novel frequency-domain approach which properly resolved the challenges associated with multiple time-delays.

It is worth noting that many results above about MASs were based on the integer-order dynamics. In fact, many scholars have declared that the essential characteristic or behavior of an object in the complex environment could be better revealed by adopting fractional-order dynamics. Examples include unmanned aerial vehicles operating in an environment with the impacts of rain and wind [22], food searching with the help of the individual secretions and microbial [23], and submarine robots in the bottom of the sea with large amounts of microorganisms and viscous substances [24]. Compared to integer-order dynamics, fractional-order dynamics provided an excellent tool in the description of memory and hereditary properties [25, 26]. Moreover, authors in [27, 28] indicated that the integer-order systems were only the special examples of the fractional-order systems. Based on these facts, the research results on consensus of FOMASs with single integral in [29–34] have been continuously springing up in recent years. As we know, consensus problem of FOMASs was first proposed and investigated by Cao *et al.* [29]. Next, consensus control of FOMASs with time-delays was studied by Yang *et al.* [30, 31], where homogeneous dynamics and heterogeneous dynamics were used to illustrate the agent of system. In [32], consensus problem of linear FOMASs with input time-delay and the consensus problem of nonlinear FOMASs with input time-delay were investigated, respectively. In [33], consensus problems were studied for FOMASs with nonuniform time-delays. Meanwhile, by means of matrix theory tool, Laplace transform and graph theory tool, two delay margins were obtained as the consensus conditions. Lately, consensus of FOMASs with double integral was proposed in [35–39]. The consensus problem of FOMASs with double integral over fixed topology was studied in [35]. By applying Mittag-Leffler function, Laplace transform, and dwell time technique, consensus for FOMASs with double integral over switching topology was investigated in [36]. Based on the sliding mode estimator, consensus problem for FOMASs with double integral was studied in [37]. By means of matrix theory tool, Laplace transform, and graph theory tool, consensus problems for a FOMAS with double integral and time-delay were studied in [38]. Nevertheless, the above research results on the consensus problems of FOMASs with or without time-delays were based on the single-integral fractional-order or double-integral fractional-order dynamics. To this day, there is almost no research on consensus problems of MIFOMASs with time-delays, especially nonuniform time-delays.

Motivated by above analysis, we extend FOMASs from single-integral fractional-order dynamics to multi-integral

fractional-order ones in this paper. Consensus problems of FOMASs with multiple integral in the presence of nonuniform time-delays are studied. The main idea of this paper is to first obtain the characteristic polynomial of a MIFOMAS with imaginary eigenvalues through the model transformation of the system and then determine the stability conditions of the system according to this characteristic polynomial, so as to determine the consensus conditions of the system according to the stability conditions of the system. The consensus conditions of the MIFOMAS with nonuniform time-delays can be obtained by inequalities.

The main contributions of this paper are as follows. Firstly, we consider multi-integral fractional-order dynamics. As far as we know, this paper is the first paper that studies consensus of MIFOMASs. Just as integer-order MASs have first-order (single-integral) MASs [4–11], second-order (double-integral) MASs [12–16], and high-order (multi-integral) MASs [17–21], FOMASs also have single-integral FOMASs [29–34], double-integral FOMASs [35–39], and MIFOMASs, which makes the overall theory of FOMASs perfect from single-integral to multi-integral FOMASs. In addition, single-integral and double-integral FOMASs are the special cases of MIFOMASs. Secondly, we consider symmetric and asymmetric time-delays. The symmetric time-delays contain up to $n(n-1)/2$ different values and the asymmetric time-delays contain up to $n(n-1)$ different values when the MIFOMAS consists of n agents. Thirdly, we consider the dynamics of each agent containing multiple state variables with different fractional orders. The MIFOMAS with nonuniform time-delays consists of some agents, and each agent contains multiple state variables with different fractional orders. Finally, we derive the consensus conditions for a MIFOMAS with nonuniform time-delays.

The remainder of this article is organized as follows. In Section 2, fractional calculus and its Laplace transform are given. In Section 3, the knowledge about graph theory is shown out. In Sections 4 and 5, consensus algorithms for a MIFOMAS in the presence of nonuniform time-delays are studied. In Section 6, some numerical examples with different parameters are simulated to verify the results. Finally, conclusions are drawn out in Section 7.

2. Fractional Calculus

In [40], several different definitions of fractional calculus have been proposed, in which the Caputo fractional derivative played an important role in fractional-order systems. Because the initial value of Caputo fractional derivative has practical signification in many problems, which is commonly used in the variety of physical fields. Ergo, this paper will model the system dynamical characteristics by using Caputo derivative which is defined by

$${}^C_a D_t^\alpha x(t) = \frac{1}{\Gamma(m-\alpha)} \int_a^t \frac{x^{(m)}(\eta)}{(t-\eta)^{1+\alpha-m}} d\eta, \quad (1)$$

where $a \in \mathbb{R}$ denotes the initial value, α represents the order of the Caputo derivative, and $m - 1 < \alpha \leq m (m \in \mathbb{Z}^+)$. $\Gamma(\cdot)$ is given by

$$\Gamma(y) = \int_0^{+\infty} e^{-t} t^{y-1} dt. \quad (2)$$

If ${}^C_a D_t^\alpha x(t)$ is replaced by $x^{(\alpha)}(t)$, and the Laplace transform of $x(t)$ is represented by $X(s) = \mathcal{L}\{x(t)\} = \int_0^\infty e^{-st} x(t) dt$, then the following equation can be used to denote Laplace transform of the Caputo derivative.

$$\mathcal{L}\{x^{(\alpha)}(t)\} = \begin{cases} s^\alpha X(s) - s^{\alpha-1} x(0^-), & \alpha \in (0, 1] \\ s^\alpha X(s) - s^{\alpha-1} x(0^-) - s^{\alpha-2} x'(0^-), & \alpha \in (1, 2] \end{cases} \quad (3)$$

where $x(0^-) = \lim_{t \rightarrow 0^-} x(t)$ and $x'(0^-) = \lim_{t \rightarrow 0^-} x'(t)$.

3. Graph Theory

For a MAS with n agents, the network topology can be denoted by a graph $\mathcal{G} = (\mathcal{V}, \mathcal{E})$, where $\mathcal{V} = \{s_1, \dots, s_n\}$ and $\mathcal{E} \subseteq \mathcal{V}^2$, respectively, represent the set of nodes and the set of edges. The node indices belong to a finite index set $\mathcal{I} = \{1, 2, \dots, n\}$. The weighted adjacency matrix is denoted by $\mathcal{A} = [a_{ij}]_{n \times n}$. The element of the i -th row and the j -th column in matrix \mathcal{A} indicates the connection state between agents s_i and s_j . If nodes s_i and s_j are connected, i.e., $e_{ij} \in \mathcal{E}$, then $a_{ij} > 0$, and s_j is called a neighbor of node s_i . $N_i = \{j \in \mathcal{I}, j \neq i\}$ denotes the index set of all neighbors of agent i . If nodes s_i and s_j are connected and $a_{ij} = a_{ji}$, then \mathcal{G} is an undirected graph; otherwise the \mathcal{G} is a directed graph. In a directed graph, a directed path is a sequence of edges by $(s_1, s_2), (s_2, s_3), \dots$, where $(s_j, s_i) \in \mathcal{E}$. The directed graph has a directed spanning tree if all other nodes have directional paths from the same node. The Laplacian matrix of the graph \mathcal{G} is defined by $L = \Delta - \mathcal{A} \in \mathbb{R}^{n \times n}$, where $\Delta \triangleq \text{diag}\{deg_{out}(s_1), deg_{out}(s_2), \dots, deg_{out}(s_i), \dots, deg_{out}(s_n)\}$ is a diagonal matrix with $deg_{out}(s_i) = \sum_{j=1}^n a_{ij}$. Supposing some graphs $\mathcal{G}_1, \mathcal{G}_2, \dots, \mathcal{G}_M$ and graph \mathcal{G} consist of the same nodes, and the edge set of graph \mathcal{G} is the sum of the edge sets of other graphs $\mathcal{G}_1, \mathcal{G}_2, \dots, \mathcal{G}_M$, then there is $L = \sum_{m=1}^M L_m$, which means the Laplacian matrix of graph \mathcal{G} is the sum of other graphs' Laplacian matrix.

4. Problem Statement

There are two lemmas [41] for the later analysis.

Lemma 1. *If graph \mathcal{G} is an undirected and connected graph, then its Laplacian matrix L has one singleton zero eigenvalue and other eigenvalues are all positive; i.e., $0 = \lambda_1 < \lambda_2 \leq \lambda_3 \leq \dots \leq \lambda_n$.*

Lemma 2. *If graph \mathcal{G} is a directed graph with a spanning tree, then its Laplacian matrix L has one singleton zero eigenvalue*

and other eigenvalues have a positive real part; i.e., $\lambda_1 = 0, \text{Re}(\lambda_i) > 0 (i = 2, 3, \dots, n)$.

Consider a MIFOMAS composed of n agents. Each node in graph \mathcal{G} corresponds to each agent of the MIFOMAS. If $a_{ij} > 0$, we can think that the i -th agent can get state information from the j -th agent. The dynamics of the i -th agent of the MIFOMAS are represented by

$$\begin{aligned} x_{i_1}^{(\alpha_1)}(t) &= x_{i_2}(t), \\ x_{i_2}^{(\alpha_2)}(t) &= x_{i_3}(t), \\ &\vdots \\ x_{i_{l-1}}^{(\alpha_{l-1})}(t) &= x_{i_l}(t), \\ x_{i_l}^{(\alpha_l)}(t) &= u_i(t), \end{aligned} \quad (4)$$

$i \in \mathcal{I}$,

where $x_{i_1}(t), x_{i_2}(t), \dots, x_{i_l}(t) \in \mathbb{R}$, respectively, represent l different states of the i -th agent, $x_{i_1}^{(\alpha_1)}(t)$ is the α_1 -order Caputo derivative of $x_{i_1}(t)$, $x_{i_2}^{(\alpha_2)}(t)$ is the α_2 -order Caputo derivative of $x_{i_2}(t)$, \dots , $x_{i_l}^{(\alpha_l)}(t)$ is the α_l -order Caputo derivative of $x_{i_l}(t)$ ($\alpha_1, \alpha_2, \dots, \alpha_l \in (0, 1]$), and $u_i(t) \in \mathbb{R}$ is the control input.

Definition 3. If and only if the states of all agents in MIFOMAS (4) satisfy

$$\begin{aligned} \lim_{t \rightarrow +\infty} (x_{i_1}(t) - x_{j_1}(t)) &= 0, \\ \lim_{t \rightarrow +\infty} (x_{i_2}(t) - x_{j_2}(t)) &= 0, \\ &\vdots \\ \lim_{t \rightarrow +\infty} (x_{i_l}(t) - x_{j_l}(t)) &= 0, \end{aligned} \quad (5)$$

$i, j \in \mathcal{I}$,

then MIFOMAS (4) can reach consensus. In (5), $x_{i_1}(t), x_{i_2}(t), \dots, x_{i_l}(t) \in \mathbb{R}$, respectively, represent l different states of the i -th agent, and $x_{j_1}(t), x_{j_2}(t), \dots, x_{j_l}(t) \in \mathbb{R}$, respectively, represent l different states of the j -th agent.

In this paper, the control protocol for MIFOMAS (4) will be given by

$$\begin{aligned} u_i(t) &= - \sum_{k=1}^{l-1} P_{k+1} x_{i_{k+1}}(t) \\ &+ \sum_{j \in N_i} a_{ij} [x_{j_1}(t - \tau_{ij}) - x_{i_1}(t - \tau_{ij})], \end{aligned} \quad (6)$$

where N_i denotes the neighbors index collection of the agent i , a_{ij} is the (i, j) -th element of \mathcal{A} , $\tau_{ij} > 0$ is the time-delay which is from the j -th agent to the i -th agent, and $P_{k+1} > 0$ are scale coefficients. If all $\tau_{ij} = \tau_{ji}$, then the time-delays are symmetrical; else the time-delays are asymmetrical. The symmetric time-delays and the asymmetric time-delays are two different forms of nonuniform time-delays. For ease of analysis, we define that τ_m denote M different time-delays of MIFOMAS (4); i.e., $\tau_m \in \{\tau_{ij} : i, j \in \mathcal{S}\}$ ($m = 1, 2, \dots, M$). Then the following control protocol is provided to resolve consensus problems of MIFOMAS (4):

$$u_i(t) = -\sum_{k=1}^{l-1} P_{k+1} x_{i_{k+1}}(t) + \sum_{j \in N_i} a_{ij} [x_{j_1}(t - \tau_m) - x_{i_1}(t - \tau_m)]. \quad (7)$$

Assume the state vector of the i -th agent is $\xi_i(t) = [x_{i_1}(t), x_{i_2}(t), \dots, x_{i_l}(t)]^T \in \mathbb{R}^l$, and the joint state vector of MIFOMAS (4) consisting of n agents is $\psi(t) = [\xi_1^T(t), \xi_2^T(t), \dots, \xi_n^T(t)]^T \in \mathbb{R}^{ln}$.

If we define two matrices as follows,

$$A = \begin{bmatrix} 0 & 1 & 0 & \cdots & 0 & 0 \\ 0 & 0 & 1 & \cdots & 0 & 0 \\ \vdots & \vdots & \vdots & \ddots & \vdots & \vdots \\ 0 & 0 & 0 & \cdots & 1 & 0 \\ 0 & 0 & 0 & \cdots & 0 & 1 \\ 0 & -P_2 & -P_3 & \cdots & -P_{l-1} & -P_l \end{bmatrix} \in \mathbb{R}^{l \times l}, \quad (8)$$

and

$$B = \begin{bmatrix} 0 & 0 & \cdots & 0 \\ \vdots & \vdots & \ddots & \vdots \\ 0 & 0 & \cdots & 0 \\ 1 & 0 & \cdots & 0 \end{bmatrix} \in \mathbb{R}^{l \times l}, \quad (9)$$

then under the control protocol given by (7), the closed-loop dynamics of MIFOMAS (4) can be described as

$$\begin{aligned} & [x_{1_1}^{(\alpha_1)}(t), x_{1_2}^{(\alpha_2)}(t), \dots, x_{1_l}^{(\alpha_l)}(t), x_{2_1}^{(\alpha_1)}(t), x_{2_2}^{(\alpha_2)}(t), \dots, \\ & x_{2_l}^{(\alpha_l)}(t), \dots, x_{n_1}^{(\alpha_1)}(t), x_{n_2}^{(\alpha_2)}(t), \dots, x_{n_l}^{(\alpha_l)}(t)]^T = (I_n \\ & \otimes A) \psi(t) - \sum_{m=1}^M (L_m \otimes B) \cdot \psi(t - \tau_m). \end{aligned} \quad (10)$$

5. Main Results

Theorem 4. Suppose that a FOMAS with multiple integral is given by MIFOMAS (4) whose corresponding network topology \mathcal{G} satisfies Lemma 1. Define the following functions:

$$\begin{aligned} F_l(\omega) &= -\sum_{k=1}^l (-j\omega)^{\sum_{i=1}^k \alpha_i} P_{k+1}, \\ \theta_l(\omega) &= \arg [F_l(\omega)] = \arg \left[-\sum_{k=1}^l (-j\omega)^{\sum_{i=1}^k \alpha_i} P_{k+1} \right] \\ &= \arctan R_l(\omega), \\ T_l(\omega) &= \frac{1}{\omega} \theta_l(\omega), \end{aligned} \quad (11)$$

where $l \in \{1, 2, 3, 4, 5, 6\}$, $R_l(\omega) \triangleq \text{Im}[F_l(\omega)]/\text{Re}[F_l(\omega)] = \tan[\theta_l(\omega)]$, and $\text{Re}[F_l(\omega)]$ and $\text{Im}[F_l(\omega)]$, respectively, denote the real part and the imaginary part of $F_l(\omega)$.

If all $\tau_m < \bar{\tau} = T_l(\bar{\omega}) = (1/\bar{\omega})\theta_l(\bar{\omega})$ for the MIFOMAS (10) with symmetric time-delays, then the control protocol (7) can resolve the consensus problem of the MIFOMAS (10) with symmetric time-delays, and on the contrary, then the control protocol (7) can not resolve the consensus problem of the MIFOMAS (10) with symmetric time-delays. The value of $\bar{\omega}$ corresponding to l in $T_l(\bar{\omega})$ is determined by the following equation:

$$|F_l(\bar{\omega})| = \lambda_n, \quad l \in \{1, 2, 3, 4, 5, 6\}, \quad (12)$$

where $|F_l(\omega)|$ is the modulus of $F_l(\omega)$ and λ_n is the maximum eigenvalue of L .

Proof. We shall apply the frequency-domain method to analyze the MIFOMAS (10) with symmetric time-delays, and we can get

$$\begin{aligned} & \left\{ I_n \otimes \begin{bmatrix} s^{\alpha_1} & 0 & \cdots & 0 & 0 \\ 0 & s^{\alpha_2} & \cdots & 0 & 0 \\ \vdots & \vdots & \ddots & \vdots & \vdots \\ 0 & 0 & \cdots & s^{\alpha_{l-1}} & 0 \\ 0 & 0 & \cdots & 0 & s^{\alpha_l} \end{bmatrix} \right\} \Psi(s) \\ & - \left\{ I_n \otimes \begin{bmatrix} s^{\alpha_1-1} & 0 & \cdots & 0 & 0 \\ 0 & s^{\alpha_2-1} & \cdots & 0 & 0 \\ \vdots & \vdots & \ddots & \vdots & \vdots \\ 0 & 0 & \cdots & s^{\alpha_{l-1}-1} & 0 \\ 0 & 0 & \cdots & 0 & s^{\alpha_l-1} \end{bmatrix} \right\} \psi(0^-) \end{aligned}$$

$$\begin{aligned}
& - (I_n \otimes A) \Psi(s) + \sum_{m=1}^M (L_m \otimes B) e^{-s\tau_m} \Psi(s) = 0, \\
& \Psi(s) = \mathcal{R} \Psi(0^-) G_{\tau_m}^{-1}(s),
\end{aligned} \tag{13}$$

where $\Psi(s)$ is the Laplace transform of $\psi(t)$, $\psi(0^-)$ is the initial value of $\psi(t)$,

$$\mathcal{R} = I_n \otimes \begin{bmatrix} s^{\alpha_1-1} & 0 & \cdots & 0 & 0 \\ 0 & s^{\alpha_2-1} & \cdots & 0 & 0 \\ \vdots & \vdots & \ddots & \vdots & \vdots \\ 0 & 0 & \cdots & s^{\alpha_{l-1}-1} & 0 \\ 0 & 0 & \cdots & 0 & s^{\alpha_l-1} \end{bmatrix}, \tag{14}$$

and

$$\begin{aligned}
G_{\tau_m}(s) = & \left\{ I_n \otimes \begin{bmatrix} s^{\alpha_1} & 0 & \cdots & 0 & 0 \\ 0 & s^{\alpha_2} & \cdots & 0 & 0 \\ \vdots & \vdots & \ddots & \vdots & \vdots \\ 0 & 0 & \cdots & s^{\alpha_{l-1}} & 0 \\ 0 & 0 & \cdots & 0 & s^{\alpha_l} \end{bmatrix} \right. \\
& - \left. \begin{bmatrix} 0 & 1 & 0 & \cdots & 0 \\ 0 & 0 & 1 & \cdots & 0 \\ \vdots & \vdots & \vdots & \ddots & \vdots \\ 0 & 0 & 0 & \cdots & 1 \\ 0 & -P_2 & -P_3 & \cdots & -P_l \end{bmatrix} \right. \\
& \left. + \sum_{m=1}^M (L_m \otimes B) e^{-s\tau_m} \right\}. \tag{15}
\end{aligned}$$

Motivated by the stability analysis of a fractional-order system in [42], we can study consensus of the MIFOMAS (10) with symmetric time-delays by analyzing the characteristic eigenvalues' position of the characteristic polynomial $\det[G_{\tau_m}(s)]$ of the MIFOMAS (10) with symmetric time-delays. Specifically, consensus of the MIFOMAS (10) without delays (all $\tau_m = 0$) is necessary for consensus of the MIFOMAS (10) with symmetric time-delays; that is to say, in this case the characteristic eigenvalues of $\det[G_{\tau_m}(s)]$ of the

MIFOMAS (10) with symmetric time-delays are all situated in the left half plane (LHP) of the complex plane, and as τ_m increases continuously from zero, the characteristic eigenvalue of $\det[G_{\tau_m}(s)]$ of the MIFOMAS (10) with symmetric time-delays will change continuously from the LHP to the right half plane (RHP) of the complex plane. Once the characteristic eigenvalue of $\det[G_{\tau_m}(s)]$ of the MIFOMAS (10) with symmetric time-delays reaches the RHP of the complex plane through the imaginary axis, the MIFOMAS (10) with symmetric time-delays will be unstable and can not achieve consensus. Ergo, we only need to consider the critical time-delay when the nonzero characteristic eigenvalue of $\det[G_{\tau_m}(s)]$ of the MIFOMAS (10) with symmetric time-delays is just situated on the imaginary axis for the first time as τ_m increases continuously from zero, and the corresponding time-delay is just the delay margin $\bar{\tau}$ of the MIFOMAS (10) with symmetric time-delays.

Assume $s = -j\omega \neq 0$ is the characteristic eigenvalue of $\det[G_{\tau_m}(s)]$ of the MIFOMAS (10) with symmetric time-delays on the imaginary axis, $u = u_1 \otimes [1, 0, \dots, 0, 0]^T + u_2 \otimes [0, 1, 0, \dots, 0]^T + \cdots + u_{l-1} \otimes [0, \dots, 0, 1, 0]^T + u_l \otimes [0, \dots, 0, 0, 1]^T$ is the corresponding eigenvector, and $\|u\| = 1$, $u_1, u_2, \dots, u_{l-1}, u_l \in \mathbb{C}^n$; we have the following equations:

$$\begin{aligned}
& \left\{ I_n \right. \\
& \otimes \left\{ \begin{bmatrix} (-j\omega)^{\alpha_1} & 0 & \cdots & 0 & 0 \\ 0 & (-j\omega)^{\alpha_2} & \cdots & 0 & 0 \\ \vdots & \vdots & \ddots & \vdots & \vdots \\ 0 & 0 & \cdots & (-j\omega)^{\alpha_{l-1}} & 0 \\ 0 & 0 & \cdots & 0 & (-j\omega)^{\alpha_l} \end{bmatrix} \right. \\
& - \left. \begin{bmatrix} 0 & 1 & 0 & \cdots & 0 \\ 0 & 0 & 1 & \cdots & 0 \\ \vdots & \vdots & \vdots & \ddots & \vdots \\ 0 & 0 & 0 & \cdots & 1 \\ 0 & -P_2 & -P_3 & \cdots & -P_l \end{bmatrix} \right\} \\
& \left. + \sum_{m=1}^M (L_m \otimes B) e^{-s\tau_m} \right\} u = 0,
\end{aligned}$$

$$\left\{ \begin{array}{l} I_n \\ \otimes \left[\begin{array}{cccccc} (-j\omega)^{\alpha_1} & -1 & 0 & \cdots & 0 \\ 0 & (-j\omega)^{\alpha_2} & -1 & \cdots & 0 \\ \vdots & \vdots & \vdots & \ddots & \vdots \\ 0 & 0 & 0 & \cdots & -1 \\ 0 & P_2 & P_3 & \cdots & P_l + (-j\omega)^{\alpha_l} \end{array} \right] \\ + \sum_{m=1}^M (L_m \otimes B) e^{-s\tau_m} \end{array} \right\} u = 0,$$

$$\underbrace{\{I_n \otimes \Omega\} u}_{(1)} + \underbrace{\left\{ \sum_{m=1}^M (L_m \otimes B) e^{j\omega\tau_m} \right\} u}_{(2)} = 0,$$

$$\begin{aligned}
(1) &= \{I_n \otimes \Omega\} u = I_n u_1 \otimes (\Omega [1, 0, \dots, 0]^T) + I_n u_2 \\
&\otimes (\Omega [0, 1, 0, \dots, 0]^T) + I_n u_3 \\
&\otimes (\Omega [0, 0, 1, 0, \dots, 0]^T) + \cdots + I_n u_{l-1} \\
&\otimes (\Omega [0, 0, \dots, 0, 1, 0]^T) + I_n u_l \\
&\otimes (\Omega [0, \dots, 0, 1]^T) = I_n u_1 \otimes [(-j\omega)^{\alpha_1}, 0, \dots, 0]^T \\
&+ I_n u_2 \otimes [-1, (-j\omega)^{\alpha_2}, 0, \dots, 0, P_2]^T + I_n u_3 \otimes [0, \\
&-1, (-j\omega)^{\alpha_3}, 0, \dots, 0, P_3]^T + \cdots + I_n u_{l-1} \otimes [0, \dots, \\
&0, -1, (-j\omega)^{\alpha_{l-1}}, P_{l-1}]^T + I_n u_l \otimes [0, \dots, 0, -1, \\
&(-j\omega)^{\alpha_l} + P_l]^T = I_n \otimes [(-j\omega)^{\alpha_1} u_1, 0, \dots, 0]^T + I_n \\
&\otimes [-u_2, (-j\omega)^{\alpha_2} u_2, 0, \dots, 0, P_2 u_2]^T + I_n \otimes [0, \\
&-u_3, (-j\omega)^{\alpha_3} u_3, 0, \dots, 0, P_3 u_3]^T + \cdots + I_n \otimes [0, \\
&\dots, 0, -u_{l-1}, (-j\omega)^{\alpha_{l-1}} u_{l-1}, P_{l-1} u_{l-1}]^T + I_n \otimes [0, \dots,
\end{aligned}$$

$$\begin{aligned}
&0, -u_l, ((-j\omega)^{\alpha_l} + P_l) u_l]^T = I_n \otimes [(-j\omega)^{\alpha_1} u_1 \\
&- u_2, (-j\omega)^{\alpha_2} u_2 - u_3, \dots, (-j\omega)^{\alpha_{l-1}} u_{l-1} - u_l, P_2 u_2 \\
&+ P_3 u_3 + \cdots + P_{l-1} u_{l-1} + P_l u_l + (-j\omega)^{\alpha_l} u_l]^T, \\
&= [I_n ((-j\omega)^{\alpha_1} u_1 - u_2), I_n ((-j\omega)^{\alpha_2} u_2 - u_3), \dots, \\
&I_n ((-j\omega)^{\alpha_{l-1}} u_{l-1} - u_l), I_n (P_2 u_2 + P_3 u_3 + \cdots \\
&+ P_{l-1} u_{l-1} + P_l u_l + (-j\omega)^{\alpha_l} u_l)]^T,
\end{aligned} \tag{17}$$

$$\begin{aligned}
(2) &= \left\{ \sum_{m=1}^M (L_m \otimes B) e^{j\omega\tau_m} \right\} u = \sum_{m=1}^M (L_m \otimes B) u e^{j\omega\tau_m} \\
&= \sum_{m=1}^M \{ (L_m u_1) \otimes (B [1, 0, \dots, 0]^T) + (L_m u_2) \\
&\otimes (B [0, 1, 0, \dots, 0]^T) + \cdots + (L_m u_{l-1}) \\
&\otimes (B [0, 0, \dots, 0, 1, 0]^T) + (L_m u_l) \\
&\otimes (B [0, \dots, 0, 1]^T) \} e^{j\omega\tau_m} = \sum_{m=1}^M \{ (L_m u_1) \\
&\otimes ([0, 0, \dots, 0, 1]^T) + (L_m u_2) \otimes ([0, 0, 0, \dots, 0]^T) \\
&+ \cdots + (L_m u_{l-1}) \otimes ([0, 0, \dots, 0, 0]^T) + (L_m u_l) \\
&\otimes ([0, \dots, 0, 0]^T) \} e^{j\omega\tau_m} = \sum_{m=1}^M (L_m \otimes I_l) [(u_1 \\
&\otimes [0, 0, \dots, 0, 1]^T) + (u_2 \otimes [0, 0, \dots, 0, 0]^T) + \cdots \\
&+ (u_{l-1} \otimes [0, 0, \dots, 0, 0]^T) + (u_l \\
&\otimes [0, 0, \dots, 0, 0]^T)] e^{j\omega\tau_m} = \sum_{m=1}^M (L_m \otimes I_l) \\
&\cdot [0, 0, \dots, 0, u_1]^T e^{j\omega\tau_m} = \left[0, 0, \dots, 0, \right. \\
&\left. \sum_{m=1}^M (L_m \otimes I_l) u_1 e^{j\omega\tau_m} \right]^T.
\end{aligned} \tag{18}$$

Because of (1) + (2) = 0, we have

$$\begin{aligned}
I_n ((-j\omega)^{\alpha_1} u_1 - u_2) &= 0, \\
I_n ((-j\omega)^{\alpha_2} u_2 - u_3) &= 0,
\end{aligned}$$

$$\begin{aligned}
& \vdots \\
& I_n \left((-j\omega)^{\alpha_{l-1}} u_{l-1} - u_l \right) = 0, \\
& I_n \left[P_2 u_2 + P_3 u_3 + \cdots + P_{l-1} u_{l-1} + \left(P_l + (-j\omega)^{\alpha_l} \right) u_l \right] \\
& + \sum_{m=1}^M (L_m \otimes I_l) u_1 e^{j\omega\tau_m} = 0,
\end{aligned} \tag{19}$$

and it yields that

$$\begin{aligned}
u_2 &= (-j\omega)^{\alpha_1} u_1, \\
u_3 &= (-j\omega)^{\alpha_2} u_2, \\
& \vdots \\
u_l &= (-j\omega)^{\alpha_{l-1}} u_{l-1}, \\
\sum_{m=1}^M (L_m \otimes I_l) u_1 e^{j\omega\tau_m} &= - \left[P_2 u_2 + P_3 u_3 + \cdots \right. \\
& \left. + P_{l-1} u_{l-1} + \left(P_l + (-j\omega)^{\alpha_l} \right) u_l \right].
\end{aligned} \tag{20}$$

According to (20), we have

$$\begin{aligned}
\sum_{m=1}^M (L_m \otimes I_l) u_1 e^{j\omega\tau_m} &= - \left[P_2 (-j\omega)^{\alpha_1} \right. \\
& + P_3 (-j\omega)^{\alpha_2 + \alpha_1} + \cdots + P_{l-1} (-j\omega)^{\alpha_{l-2} + \alpha_{l-3} + \cdots + \alpha_1} \\
& \left. + P_l (-j\omega)^{\alpha_{l-1} + \alpha_{l-2} + \cdots + \alpha_1} + (-j\omega)^{\alpha_l + \alpha_{l-1} + \cdots + \alpha_1} \right] u_1,
\end{aligned} \tag{21}$$

then we can multiply both sides of (21) by u^H (the conjugate transpose of u); the following equation can be obtained:

$$\begin{aligned}
\sum_{m=1}^M \frac{u^H (L_m \otimes I_l) u_1}{u^H u_1} e^{j\omega\tau_m} &= - \left[P_2 (-j\omega)^{\alpha_1} \right. \\
& + P_3 (-j\omega)^{\alpha_2 + \alpha_1} + \cdots + P_{l-1} (-j\omega)^{\alpha_{l-2} + \alpha_{l-3} + \cdots + \alpha_1} \\
& \left. + P_l (-j\omega)^{\alpha_{l-1} + \alpha_{l-2} + \cdots + \alpha_1} + (-j\omega)^{\alpha_l + \alpha_{l-1} + \cdots + \alpha_1} \right] \\
&= - \sum_{k=1}^l (-j\omega)^{\sum_{i=1}^k \alpha_i} P_{k+1},
\end{aligned} \tag{22}$$

where $l \geq 1, P_{l+1} = 1$.

Due to

$$u = [u_1, u_2, u_3, \dots, u_l]^T = [u_1, (-j\omega)^{\alpha_1} u_1, (-j\omega)^{\alpha_1 + \alpha_2}$$

$$\cdot u_1, \dots, (-j\omega)^{\alpha_{l-1} + \alpha_{l-2} + \cdots + \alpha_1} u_1]^T,$$

$$u_1 = \frac{u}{\left\{ [1, (-j\omega)^{\alpha_1}, (-j\omega)^{\alpha_1 + \alpha_2}, \dots, (-j\omega)^{\alpha_{l-1} + \alpha_{l-2} + \cdots + \alpha_1}]^T \right\}}, \tag{23}$$

(22) can be simplified to

$$\begin{aligned}
\sum_{m=1}^M \frac{u^H (L_m \otimes I_l) u_1}{u^H u_1} e^{j\omega\tau_m} &= \sum_{m=1}^M \frac{u^H (L_m \otimes I_l) u}{u^H u} e^{j\omega\tau_m} \\
&= - \sum_{k=1}^l (-j\omega)^{\sum_{i=1}^k \alpha_i} P_{k+1} \triangleq F_l(\omega),
\end{aligned} \tag{24}$$

where $l \geq 1, P_{l+1} = 1$.

Let $u^H (L_m \otimes I_l) u / (u^H u) = a_m$; we take modulus of both sides of (24). According to Lemma 1, we can get the following inequality:

$$\begin{aligned}
M_l(\omega) = |F_l(\omega)| &= \left| \sum_{m=1}^M a_m e^{j\omega\tau_m} \right| \leq \left| \sum_{m=1}^M a_m \right| \\
&= \frac{u^H (L \otimes I_l) u}{u^H u} \leq M_l(\bar{\omega}) = |F_l(\bar{\omega})| = \lambda_n.
\end{aligned} \tag{25}$$

It is obvious that $M_l(\omega)$ is an increasing function for $\omega > 0$, and if $\omega \leq \bar{\omega}$, we can get $M_l(\omega) \leq M_l(\bar{\omega}) = |F_l(\bar{\omega})| = \lambda_n$; that is, inequality (25) is true.

According to (24), we can get

$$\begin{aligned}
\arg [F_l(\omega)] &= \arg \left(\sum_{m=1}^M a_m e^{j\omega\tau_m} \right) \triangleq \theta_l(\omega), \\
&= \arctan R_l(\omega),
\end{aligned} \tag{26}$$

where $\theta_l(\omega)$ is the principal value of the argument of $F_l(\omega)$, $R_l(\omega) \triangleq \text{Im}[F_l(\omega)] / \text{Re}[F_l(\omega)] = \tan[\theta_l(\omega)]$, and $\text{Re}[F_l(\omega)]$ and $\text{Im}[F_l(\omega)]$, respectively, denote the real part and the imaginary part of $F_l(\omega)$.

According to (26), it is easy to obtain that

$$\theta_l(\omega) = \arg \left(\sum_{m=1}^M a_m e^{j\omega\tau_m} \right) \leq \max \{ \omega\tau_m \}. \tag{27}$$

Consider a FOMAS with single integral; we have $F_1(\omega) = -(-j\omega)^{\alpha_1} P_2 = \omega^{\alpha_1} e^{j(\pi(2-\alpha_1)/2)} P_2$. It is apparent that $\theta_1(\omega) = \pi(2 - \alpha_1)/2$, and $M_1(\omega) = \omega^{\alpha_1} P_2 (P_2 = 1)$. According to (25), we should only consider $\omega \leq \bar{\omega} = \lambda_n^{(1/\alpha_1)}$, and if all $\tau_m < \bar{\tau} = T_1(\bar{\omega}) = T_1[\lambda_n^{(1/\alpha_1)}] = (1/\bar{\omega})\theta_1(\bar{\omega}) = \pi(2 - \alpha_1)/[2\lambda_n^{(1/\alpha_1)}]$, then $\omega\tau_m < \lambda_n^{(1/\alpha_1)}\bar{\tau} = \lambda_n^{(1/\alpha_1)}T_1[\lambda_n^{(1/\alpha_1)}] = \pi(2 - \alpha_1)/2 = \theta_1(\omega)$, which contradicts to (27). Therefore, when all $\tau_m < \bar{\tau}$, the characteristic eigenvalues of $\det[G_{\tau_m}(s)]$

of the MIFOMAS (10) with symmetric time-delays are all situated in the LHP and the FOMAS with single integral will remain stable and can achieve consensus. On the contrary, the FOMAS with single integral will not remain stable and can not achieve consensus. Theorem 4 is proven for $l = 1$.

In the following, the FOMAS with multiple integral (double integral to sextuple integral) shall be analyzed step by step. For convenience of analysis, we first need to define some symbolic parameters:

$$\begin{aligned}
z_1 &= \omega^{2\alpha_1} P_2^2, \\
z_2 &= \omega^{2(\alpha_1+\alpha_2)} P_3^2, \\
z_3 &= 2\omega^{(2\alpha_1+\alpha_2)} \cos \frac{\pi\alpha_2}{2} P_2 P_3, \\
z_4 &= 2\omega^{(2\alpha_1+\alpha_2+\alpha_3)} \cos \frac{\pi(\alpha_2+\alpha_3)}{2} P_2 P_4, \\
z_5 &= 2\omega^{(2\alpha_1+\alpha_2+\alpha_3+\alpha_4)} \cos \frac{\pi(\alpha_2+\alpha_3+\alpha_4)}{2} P_2 P_5, \\
z_6 &= 2\omega^{(2\alpha_1+\alpha_2+\alpha_3+\alpha_4+\alpha_5)} \cos \frac{\pi(\alpha_2+\alpha_3+\alpha_4+\alpha_5)}{2} \\
&\quad \cdot P_2 P_6, \\
z_7 &= 2\omega^{(2\alpha_1+\alpha_2+\alpha_3+\alpha_4+\alpha_5+\alpha_6)} \\
&\quad \cdot \cos \frac{\pi(\alpha_2+\alpha_3+\alpha_4+\alpha_5+\alpha_6)}{2} P_2 P_7, \\
z_8 &= 2\omega^{(2\alpha_1+2\alpha_2+\alpha_3)} \cos \frac{\pi\alpha_3}{2} P_3 P_4, \\
z_9 &= 2\omega^{(2\alpha_1+2\alpha_2+\alpha_3+\alpha_4)} \cos \frac{\pi(\alpha_3+\alpha_4)}{2} P_3 P_5, \\
z_{10} &= 2\omega^{(2\alpha_1+2\alpha_2+\alpha_3+\alpha_4+\alpha_5)} \cos \frac{\pi(\alpha_3+\alpha_4+\alpha_5)}{2} P_3 P_6, \\
z_{11} &= 2\omega^{(2\alpha_1+2\alpha_2+\alpha_3+\alpha_4+\alpha_5+\alpha_6)} \cos \frac{\pi(\alpha_3+\alpha_4+\alpha_5+\alpha_6)}{2} \\
&\quad \cdot P_3 P_7, \\
z_{12} &= \omega^{2(\alpha_1+\alpha_2+\alpha_3)} P_4^2, \\
z_{13} &= 2\omega^{(2\alpha_1+2\alpha_2+2\alpha_3+\alpha_4)} \cos \frac{\pi\alpha_4}{2} P_4 P_5, \\
z_{14} &= 2\omega^{(2\alpha_1+2\alpha_2+2\alpha_3+\alpha_4+\alpha_5)} \cos \frac{\pi(\alpha_4+\alpha_5)}{2} P_4 P_6, \\
z_{15} &= 2\omega^{(2\alpha_1+2\alpha_2+2\alpha_3+\alpha_4+\alpha_5+\alpha_6)} \cos \frac{\pi(\alpha_4+\alpha_5+\alpha_6)}{2} \\
&\quad \cdot P_4 P_7,
\end{aligned}$$

$$\begin{aligned}
z_{16} &= \omega^{2(\alpha_1+\alpha_2+\alpha_3+\alpha_4)} P_5^2, \\
z_{17} &= 2\omega^{(2\alpha_1+2\alpha_2+2\alpha_3+2\alpha_4+\alpha_5)} \cos \frac{\pi\alpha_5}{2} P_5 P_6, \\
z_{18} &= 2\omega^{(2\alpha_1+2\alpha_2+2\alpha_3+2\alpha_4+\alpha_5+\alpha_6)} \cos \frac{\pi(\alpha_5+\alpha_6)}{2} P_5 P_7, \\
z_{19} &= \omega^{2(\alpha_1+\alpha_2+\alpha_3+\alpha_4+\alpha_5)} P_6^2, \\
z_{20} &= 2\omega^{(2\alpha_1+2\alpha_2+2\alpha_3+2\alpha_4+2\alpha_5+\alpha_6)} \cos \frac{\pi\alpha_6}{2} P_6 P_7, \\
z_{21} &= \omega^{2(\alpha_1+\alpha_2+\alpha_3+\alpha_4+\alpha_5+\alpha_6)} P_7^2,
\end{aligned} \tag{28}$$

and

$$\begin{aligned}
d_1 &= \alpha_2 \omega^{(2\alpha_1+\alpha_2-1)} P_2 P_3 \sin \frac{\pi\alpha_2}{2}, \\
d_2 &= (\alpha_2+\alpha_3) \omega^{(2\alpha_1+\alpha_2+\alpha_3-1)} P_2 P_4 \sin \frac{\pi(\alpha_2+\alpha_3)}{2}, \\
d_3 &= (\alpha_2+\alpha_3+\alpha_4) \omega^{(2\alpha_1+\alpha_2+\alpha_3+\alpha_4-1)} P_2 P_5 \\
&\quad \cdot \sin \frac{\pi(\alpha_2+\alpha_3+\alpha_4)}{2}, \\
d_4 &= (\alpha_2+\alpha_3+\alpha_4+\alpha_5) \omega^{(2\alpha_1+\alpha_2+\alpha_3+\alpha_4+\alpha_5-1)} \cdot P_2 P_6 \\
&\quad \cdot \sin \frac{\pi(\alpha_2+\alpha_3+\alpha_4+\alpha_5)}{2}, \\
d_5 &= (\alpha_2+\alpha_3+\alpha_4+\alpha_5+\alpha_6) \omega^{(2\alpha_1+\alpha_2+\alpha_3+\alpha_4+\alpha_5+\alpha_6-1)} \\
&\quad \cdot P_2 P_7 \sin \frac{\pi(\alpha_2+\alpha_3+\alpha_4+\alpha_5+\alpha_6)}{2}, \\
d_6 &= \alpha_3 \omega^{(2\alpha_1+2\alpha_2+\alpha_3-1)} P_3 P_4 \sin \frac{\pi\alpha_3}{2}, \\
d_7 &= (\alpha_3+\alpha_4) \omega^{(2\alpha_1+2\alpha_2+\alpha_3+\alpha_4-1)} P_3 P_5 \sin \frac{\pi(\alpha_3+\alpha_4)}{2}, \\
d_8 &= (\alpha_3+\alpha_4+\alpha_5) \omega^{(2\alpha_1+2\alpha_2+\alpha_3+\alpha_4+\alpha_5-1)} \cdot P_3 P_6 \\
&\quad \cdot \sin \frac{\pi(\alpha_3+\alpha_4+\alpha_5)}{2}, \\
d_9 &= (\alpha_3+\alpha_4+\alpha_5+\alpha_6) \omega^{(2\alpha_1+2\alpha_2+\alpha_3+\alpha_4+\alpha_5+\alpha_6-1)} \\
&\quad \cdot P_3 P_7 \sin \frac{\pi(\alpha_3+\alpha_4+\alpha_5+\alpha_6)}{2}, \\
d_{10} &= \alpha_4 \omega^{(2\alpha_1+2\alpha_2+2\alpha_3+\alpha_4-1)} P_4 P_5 \sin \frac{\pi\alpha_4}{2}, \\
d_{11} &= (\alpha_4+\alpha_5) \omega^{(2\alpha_1+2\alpha_2+2\alpha_3+\alpha_4+\alpha_5-1)} P_4 P_6
\end{aligned}$$

$$\begin{aligned}
& \cdot \sin \frac{\pi(\alpha_4 + \alpha_5)}{2}, \\
d_{12} &= (\alpha_4 + \alpha_5 + \alpha_6) \omega^{(2\alpha_1 + 2\alpha_2 + 2\alpha_3 + \alpha_4 + \alpha_5 + \alpha_6 - 1)} \cdot P_4 P_7 \\
& \cdot \sin \frac{\pi(\alpha_4 + \alpha_5 + \alpha_6)}{2}, \\
d_{13} &= \alpha_5 \omega^{(2\alpha_1 + 2\alpha_2 + 2\alpha_3 + 2\alpha_4 + \alpha_5 - 1)} P_5 P_6 \sin \frac{\pi\alpha_5}{2}, \\
d_{14} &= (\alpha_5 + \alpha_6) \omega^{(2\alpha_1 + 2\alpha_2 + 2\alpha_3 + 2\alpha_4 + \alpha_5 + \alpha_6 - 1)} P_5 P_7 \\
& \cdot \sin \frac{\pi(\alpha_5 + \alpha_6)}{2}, \\
d_{15} &= \alpha_6 \omega^{(2\alpha_1 + 2\alpha_2 + 2\alpha_3 + 2\alpha_4 + 2\alpha_5 + \alpha_6 - 1)} P_6 P_7 \sin \frac{\pi\alpha_6}{2}.
\end{aligned} \tag{29}$$

For the FOMAS with double integral,

$$\begin{aligned}
F_2(\omega) &= -\sum_{k=1}^2 (-j\omega)^{\sum_{i=1}^k \alpha_i} P_{k+1} = -\left[(-j\omega)^{\alpha_1} P_2 \right. \\
& \left. + (-j\omega)^{\alpha_1 + \alpha_2} P_3\right] = \omega^{\alpha_1} e^{j(\pi(2-\alpha_1)/2)} P_2
\end{aligned}$$

$$\begin{aligned}
& + \omega^{\alpha_1 + \alpha_2} e^{j(\pi(2-\alpha_1-\alpha_2)/2)} P_3 = \left[\omega^{\alpha_1} P_2 \cos \frac{\pi(2-\alpha_1)}{2} \right. \\
& \left. + \omega^{(\alpha_1 + \alpha_2)} P_3 \cos \frac{\pi(2-\alpha_1-\alpha_2)}{2} \right] \\
& + j \left[\omega^{\alpha_1} P_2 \sin \frac{\pi(2-\alpha_1)}{2} \right. \\
& \left. + \omega^{(\alpha_1 + \alpha_2)} P_3 \sin \frac{\pi(2-\alpha_1-\alpha_2)}{2} \right] = \text{Re} [F_2(\omega)] \\
& + j \text{Im} [F_2(\omega)].
\end{aligned} \tag{30}$$

$$\begin{aligned}
[M_2(\omega)]^2 &= |F_2(\omega)|^2 = \omega^{2\alpha_1} P_2^2 + \omega^{2(\alpha_1 + \alpha_2)} P_3^2 \\
& + 2\omega^{(2\alpha_1 + \alpha_2)} \cos \frac{\pi\alpha_2}{2} P_2 P_3 = z_1 + z_2 + z_3.
\end{aligned} \tag{31}$$

Because of $R_2(\omega) = \text{Im}[F_2(\omega)]/\text{Re}[F_2(\omega)]$, we can get the first derivative of $R_2(\omega)$:

$$R_2'(\omega) = -\frac{[\alpha_2 \omega^{2\alpha_1 + \alpha_2 - 1} P_2 P_3 \sin(\pi\alpha_2/2)]}{[\omega^{\alpha_1} P_2 \cos(\pi(2-\alpha_1)/2) + \omega^{(\alpha_1 + \alpha_2)} P_3 \cos(\pi(2-\alpha_1-\alpha_2)/2)]^2} = -\frac{d_1}{\{\text{Re}[F_2(\omega)]\}^2} < 0. \tag{32}$$

For the FOMAS with triple integral,

$$\begin{aligned}
F_3(\omega) &= -\sum_{k=1}^3 (-j\omega)^{\sum_{i=1}^k \alpha_i} P_{k+1} = -\left[(-j\omega)^{\alpha_1} P_2 \right. \\
& \left. + (-j\omega)^{\alpha_1 + \alpha_2} P_3 + (-j\omega)^{\alpha_1 + \alpha_2 + \alpha_3} P_4\right] \\
& = \omega^{\alpha_1} e^{j(\pi(2-\alpha_1)/2)} P_2 + \omega^{\alpha_1 + \alpha_2} e^{j(\pi(2-\alpha_1-\alpha_2)/2)} P_3 \\
& + \omega^{(\alpha_1 + \alpha_2 + \alpha_3)} e^{j(\pi(2-\alpha_1-\alpha_2-\alpha_3)/2)} P_4 \\
& = \left[\omega^{\alpha_1} P_2 \cos \frac{\pi(2-\alpha_1)}{2} \right. \\
& \left. + \omega^{(\alpha_1 + \alpha_2)} P_3 \cos \frac{\pi(2-\alpha_1-\alpha_2)}{2} \right. \\
& \left. + \omega^{(\alpha_1 + \alpha_2 + \alpha_3)} P_4 \cos \frac{\pi(2-\alpha_1-\alpha_2-\alpha_3)}{2} \right]
\end{aligned}$$

$$\begin{aligned}
& + j \left[\omega^{\alpha_1} P_2 \sin \frac{\pi(2-\alpha_1)}{2} \right. \\
& \left. + \omega^{(\alpha_1 + \alpha_2)} P_3 \sin \frac{\pi(2-\alpha_1-\alpha_2)}{2} \right. \\
& \left. + \omega^{(\alpha_1 + \alpha_2 + \alpha_3)} P_4 \sin \frac{\pi(2-\alpha_1-\alpha_2-\alpha_3)}{2} \right] \\
& = \text{Re} [F_3(\omega)] + j \text{Im} [F_3(\omega)],
\end{aligned} \tag{33}$$

$$\begin{aligned}
[M_3(\omega)]^2 &= |F_3(\omega)|^2 = \omega^{2\alpha_1} P_2^2 + \omega^{2(\alpha_1 + \alpha_2)} P_3^2 \\
& + 2\omega^{(2\alpha_1 + \alpha_2)} \cos \frac{\pi\alpha_2}{2} P_2 P_3 + 2\omega^{(2\alpha_1 + \alpha_2 + \alpha_3)} \\
& \cdot \cos \frac{\pi(\alpha_2 + \alpha_3)}{2} P_2 P_4 + 2\omega^{(2\alpha_1 + 2\alpha_2 + \alpha_3)} \cos \frac{\pi\alpha_3}{2} P_3 P_4 \\
& + \omega^{2(\alpha_1 + \alpha_2 + \alpha_3)} P_4^2 = z_1 + z_2 + z_3 + z_4 + z_8 + z_{12}.
\end{aligned} \tag{34}$$

Because of $R_3(\omega) = \text{Im}[F_3(\omega)]/\text{Re}[F_3(\omega)]$, we can get the first derivative of $R_3(\omega)$:

$$\begin{aligned}
 R_3'(\omega) &= -\frac{[\alpha_2\omega^{(2\alpha_1+\alpha_2-1)}P_2P_3 \sin(\pi\alpha_2/2) + (\alpha_2 + \alpha_3)\omega^{(2\alpha_1+\alpha_2+\alpha_3-1)} \cdot P_2P_4 \sin(\pi(\alpha_2 + \alpha_3)/2) + \alpha_3\omega^{(2\alpha_1+2\alpha_2+\alpha_3-1)}P_3P_4 \sin(\pi\alpha_3/2)]}{[\omega^{\alpha_1}P_2 \cdot \cos(\pi(2 - \alpha_1)/2) + \omega^{(\alpha_1+\alpha_2)}P_3 \cos(\pi(2 - \alpha_1 - \alpha_2)/2) + \omega^{(\alpha_1+\alpha_2+\alpha_3)}P_4 \cdot \cos(\pi(2 - \alpha_1 - \alpha_2 - \alpha_3)/2)]^2} \\
 &= -\frac{(d_1 + d_2 + d_6)}{\{\text{Re}[F_3(\omega)]\}^2} < 0.
 \end{aligned} \tag{35}$$

In a similar way, the $[M_l(\omega)]^2$ and $R_l'(\omega)$ of the FOMASs with quadruple integral to sextuple integral can

be, respectively, calculated under the appropriate parameters, and they are as follows:

$$\begin{aligned}
 [M_4(\omega)]^2 &= z_1 + z_2 + z_3 + z_4 + z_5 + z_8 + z_9 + z_{12} + z_{13} + z_{16}, \\
 R_4'(\omega) &= -\frac{(d_1 + d_2 + d_3 + d_6 + d_7 + d_{10})}{\{\text{Re}[F_4(\omega)]\}^2} < 0.
 \end{aligned} \tag{36}$$

$$\begin{aligned}
 [M_5(\omega)]^2 &= z_1 + z_2 + z_3 + z_4 + z_5 + z_6 + z_8 + z_9 + z_{10} + z_{12} + z_{13} + z_{14} + z_{16} + z_{17} + z_{19}, \\
 R_5'(\omega) &= -\frac{(d_1 + d_2 + d_3 + d_4 + d_6 + d_7 + d_8 + d_{10} + d_{11} + d_{13})}{\{\text{Re}[F_5(\omega)]\}^2} < 0.
 \end{aligned} \tag{37}$$

$$\begin{aligned}
 [M_6(\omega)]^2 &= z_1 + z_2 + z_3 + z_4 + z_5 + z_6 + z_7 + z_8 + z_9 + z_{10} + z_{11} + z_{12} + z_{13} + z_{14} + z_{15} + z_{16} + z_{17} + z_{18} + z_{19} + z_{20} \\
 &\quad + z_{21},
 \end{aligned} \tag{38}$$

$$R_6'(\omega) = -\frac{(d_1 + d_2 + d_3 + d_4 + d_5 + d_6 + d_7 + d_8 + d_9 + d_{10} + d_{11} + d_{12} + d_{13} + d_{14} + d_{15})}{\{\text{Re}[F_6(\omega)]\}^2} < 0.$$

In summary, we have found that the first derivatives of $R_l(\omega)$ ($2 \leq l \leq 6$) listed above are negative values, and $R_l'(\omega) < 0$ means that $R_l(\omega) = \tan[\theta_l(\omega)]$ are monotonically decreasing with the growth of ω . Then it can be deduced that the arguments $\theta_l(\omega)$ also decrease monotonically and continuously about ω because the values of $F_l(\omega)$ vary smoothly. Evidently, we can analyze the features of $\theta_l(\omega)$ ($2 \leq l \leq 6$) together.

If $0 < \omega_1 < \omega_2$, we have $\omega_2/\omega_1 > 1$, and because the arguments $\theta_l(\omega)$ decrease monotonically and continuously about ω , we have $\theta_l(\omega_1) > \theta_l(\omega_2)$; i.e., $\theta_l(\omega_1)/\theta_l(\omega_2) > 1$. Thus,

$$\frac{T_l(\omega_1)}{T_l(\omega_2)} = \frac{\theta_l(\omega_1)}{\omega_1} \cdot \frac{\omega_2}{\theta_l(\omega_2)} = \frac{\theta_l(\omega_1)}{\theta_l(\omega_2)} \cdot \frac{\omega_2}{\omega_1} > 1, \tag{39}$$

so we can get $T_l(\omega_1) > T_l(\omega_2)$, which means $T_l(\omega)$ also decrease monotonically and continuously about ω . When $\omega \leq \bar{\omega}$, we have

$$T_l(\omega) \geq T_l(\bar{\omega}) = \bar{\tau}. \tag{40}$$

It is worth noting that inequality (40) can be obtained when the characteristic eigenvalue of $\det[G_{\tau_m}(s)]$ of the MIFOMAS (10) is $s = -j\omega \neq 0$. If we let all $\tau_m < \bar{\tau}$, then we can obtain the following inequality:

$$\begin{aligned}
 T_l(\omega) &= \frac{\theta_l(\omega)}{\omega} = \frac{\arg\left(\sum_{m=1}^M a_m e^{j\omega\tau_m}\right)}{\omega} \leq \frac{\max\{\omega\tau_m\}}{\omega} \\
 &< \frac{\omega\bar{\tau}}{\omega} = \bar{\tau}.
 \end{aligned} \tag{41}$$

Inequality (41) is in contradiction with inequality (40). Therefore, as long as all $\tau_m < \bar{\tau}$, we can ensure all the characteristic eigenvalues of $\det[G_{\tau_m}(s)]$ of the MIFOMAS (10) with symmetric time-delays are situated in the LHP, and the MIFOMAS (10) with symmetric time-delays will remain stable and can achieve consensus. On the contrary, the MIFOMAS (10) with symmetric time-delays will not be stable and can not achieve consensus. Theorem 4 is proven for $l \in \{2, 3, 4, 5, 6\}$. \square

Remark 5. Consensus of the MIFOMAS (10) without symmetric time-delays is necessary for consensus of this system with symmetric time-delays.

Remark 6. Although $l \in \{1, 2, 3, 4, 5, 6\}$ in Theorem 4 due to computational complexity, the value of l may be greater than 6 under the appropriate parameters.

Corollary 7. *If we suppose that a FOMAS with multiple integral is given by MIFOMAS (4) whose corresponding network topology \mathcal{G} satisfies Lemma 1 and $\alpha_1 = \alpha_2 = \dots = \alpha_l = 1$, then the MIFOMAS (10) with symmetric time-delays can be transformed into high-order MAS with symmetric time-delays whose dynamic model is an integer-order dynamic model and the following functions can be obtained:*

$$\begin{aligned} F_l(\omega) &= -\sum_{k=1}^l (-j\omega)^k P_{k+1}, \\ \theta_l(\omega) &= \arg[F_l(\omega)] = \arg\left[-\sum_{k=1}^l (-j\omega)^k P_{k+1}\right] \\ &= \arctan R_l(\omega), \\ T_l(\omega) &= \frac{1}{\omega}\theta_l(\omega), \end{aligned} \quad (42)$$

where $l \in \{1, 2, 3, 4, 5, 6\}$, $R_l(\omega) \triangleq \text{Im}[F_l(\omega)]/\text{Re}[F_l(\omega)] = \tan[\theta_l(\omega)]$, and $\text{Re}[F_l(\omega)]$ and $\text{Im}[F_l(\omega)]$, respectively, denote the real part and the imaginary part of $F_l(\omega)$.

For the high-order MAS with symmetric time-delays, if all τ_m satisfy $\tau_m < \bar{\tau} = T_l(\bar{\omega}) = (1/\bar{\omega})\theta_l(\bar{\omega})$, then the control protocol (7) can resolve the consensus problem for the high-order MAS with symmetric time-delays, and on the contrary, then the control protocol (7) can not resolve the consensus problem for the high-order MAS with symmetric time-delays. The value of $\bar{\omega}$ corresponding to l in $T_l(\bar{\omega})$ is determined by the following equation:

$$|F_l(\bar{\omega})| = \lambda_n, \quad l \in \{1, 2, 3, 4, 5, 6\}, \quad (43)$$

where $|F_l(\omega)|$ is the modulus of $F_l(\omega)$ and λ_n is the maximum eigenvalue of L .

Remark 8. The dynamic model and the control protocol in Corollary 7 were discussed in [21], and the conclusion in Corollary 7 is less conservative than that in [21]. The proof about Corollary 7 is the same as that of Theorem 4.

Theorem 9. *Suppose that a FOMAS with multiple integral is given by MIFOMAS (4) whose corresponding network topology \mathcal{G} satisfies Lemma 2. Define the following functions:*

$$\begin{aligned} B_l(\omega) &= -\sum_{k=1}^l (-j\omega)^{\sum_{i=1}^k \alpha_i} P_{k+1}, \\ \Theta_l(\omega) &= \arg[B_l(\omega)] = \arg\left[-\sum_{k=1}^l (-j\omega)^{\sum_{i=1}^k \alpha_i} P_{k+1}\right] \\ &= \arctan R_l(\omega), \\ \Gamma_l(\omega) &= \frac{1}{\omega}[\Theta_l(\omega) - \arg(\lambda_i)], \end{aligned} \quad (44)$$

where $l \in \{1, 2, 3, 4, 5, 6\}$, $\arg(\lambda_i) \in (-\pi/2, \pi/2)$, λ_i is the i -th eigenvalue of L , $R_l(\omega) \triangleq \text{Im}[B_l(\omega)]/\text{Re}[B_l(\omega)] = \tan[\Theta_l(\omega)]$, and $\text{Im}[B_l(\omega)]$ and $\text{Re}[B_l(\omega)]$ denote the imaginary part and real part of $B_l(\omega)$, respectively.

If all τ_m satisfy $\tau_m < \bar{\tau} = \min_{|\lambda_i| \neq 0} \{\Gamma_l(\bar{\omega}_i)\}$ for the MIFOMAS (10) with asymmetric time-delays, then the control protocol (7) can resolve the consensus problem of the MIFOMAS (10) with asymmetric time-delays, and on the contrary, then the control protocol (7) can not resolve the consensus problem of the MIFOMAS (10) with asymmetric time-delays. The value of $\bar{\omega}_i$ corresponding to l in $\Gamma_l(\bar{\omega}_i)$ is determined by the following equation:

$$|B_l(\bar{\omega}_i)| = |\lambda_i|, \quad l \in \{1, 2, 3, 4, 5, 6\}, \quad (45)$$

where $|B_l(\bar{\omega}_i)|$ is the modulus of $B_l(\bar{\omega}_i)$.

Proof. By adopting the proof method similar to Theorem 4, we suppose that $s = -j\omega \neq 0$ is the characteristic eigenvalue of $\det[G_{\tau_m}(s)]$ of the MIFOMAS (10) with asymmetric time-delays on the imaginary axis, $u = u_1 \otimes [1, 0, \dots, 0, 0]^T + u_2 \otimes [0, 1, 0, \dots, 0]^T + \dots + u_{l-1} \otimes [0, \dots, 0, 1, 0]^T + u_l \otimes [0, \dots, 0, 0, 1]^T$ is the corresponding eigenvector, and $\|u\| = 1$, $u_1, u_2, \dots, u_{l-1}, u_l \in \mathbb{C}^n$. According to Lemma 2, we can get the following equation:

$$B_l(\omega) \triangleq \sum_{m=1}^M a_m e^{j\omega\tau_m} = -\sum_{k=1}^l (-j\omega)^{\sum_{i=1}^k \alpha_i} P_{k+1}. \quad (46)$$

Take modulus of both sides of (46); $|B_l(\omega)|$ is an increasing function for $\omega > 0$; thus $\omega(|B_l(\omega)|)$ is also an increasing function for $|B_l(\omega)|$.

Calculate the principal value of the argument of (46); we have

$$\begin{aligned} \Theta_l(\omega) &\triangleq \arg[B_l(\omega)] = \arg\left[-\sum_{k=1}^l (-j\omega)^{\sum_{i=1}^k \alpha_i} P_{k+1}\right] \\ &= \arctan R_l(\omega), \end{aligned} \quad (47)$$

where $R_l(\omega) \triangleq \text{Im}[B_l(\omega)]/\text{Re}[B_l(\omega)] = \tan[\Theta_l(\omega)]$ and $\text{Im}[B_l(\omega)]$ and $\text{Re}[B_l(\omega)]$ denote the imaginary part and real part of $B_l(\omega)$, respectively.

According to the definition of $B_l(\omega)$ in (46), we have

$$\Theta_l(\omega) \leq \arg\left(\sum_{m=1}^M a_m\right) + \max(\omega\tau_m), \quad (48)$$

so there is

$$\max(\omega\tau_m) \geq \Theta_l(\omega) - \arg\left(\sum_{m=1}^M a_m\right). \quad (49)$$

Due to $\sum_{m=1}^M a_m = u^H(L \otimes I_l)u/(u^H u)$, the possible values of $\sum_{m=1}^M a_m$ must be nonzero eigenvalues of L of graph \mathcal{G} ; i.e., $\sum_{m=1}^M a_m = \lambda_i$ ($\lambda_i \neq 0$), which makes the delay margin $\bar{\tau}$ minimized. So when $|B_l(\omega)| \leq |\lambda_i|$, $\omega(|B_l(\omega)|) \leq \omega(|\lambda_i|) = \bar{\omega}_i$. If we let all $\tau_m < \bar{\tau}$, there is

$$\begin{aligned} \max(\omega\tau_m) &< \bar{\omega}_i \bar{\tau} = \bar{\omega}_i \min_{|\lambda_i| \neq 0} \{\Gamma_l(\bar{\omega}_i)\} \\ &= \min_{|\lambda_i| \neq 0} \left\{ \frac{[\Theta_l(\bar{\omega}_i) - \arg(\lambda_i)]}{\bar{\omega}_i} \right\} \bar{\omega}_i \\ &\leq \Theta_l(\omega) - \arg\left(\sum_{m=1}^M a_m\right). \end{aligned} \quad (50)$$

Inequality (50) is in contradiction with inequality (49). Therefore, as long as all $\tau_m < \bar{\tau}$, the characteristic eigenvalues of $\det[G_{\tau_m}(s)]$ of the MIFOMAS (10) with asymmetric time-delays can not reach or pass through the imaginary axis, then the MIFOMAS (10) with asymmetric time-delays will remain stable and can achieve consensus. On the contrary, the MIFOMAS (10) with asymmetric time-delays will not be stable and can not achieve consensus. Theorem 9 is proven. \square

Remark 10. Consensus of the MIFOMAS (10) without asymmetric time-delays is necessary for consensus of this system with asymmetric time-delays.

Remark 11. Although $l \in \{1, 2, 3, 4, 5, 6\}$ in Theorem 9 due to computational complexity, the value of l may be greater than 6 under the appropriate parameters.

Corollary 12. *If we suppose that a FOMAS with multiple integral is given by MIFOMAS (4) whose corresponding network topology \mathcal{G} satisfies Lemma 2 and $\alpha_1 = \alpha_2 = \dots = \alpha_l = 1$, then the MIFOMAS (10) with asymmetric time-delays can be transformed into high-order MAS with asymmetric time-delays whose dynamic model is an integer-order dynamic model and the following functions can be obtained:*

$$\begin{aligned} B_l(\omega) &= -\sum_{k=1}^l (-j\omega)^k P_{k+1}, \\ \Theta_l(\omega) &= \arg[B_l(\omega)] = \arg\left[-\sum_{k=1}^l (-j\omega)^k P_{k+1}\right] \end{aligned}$$

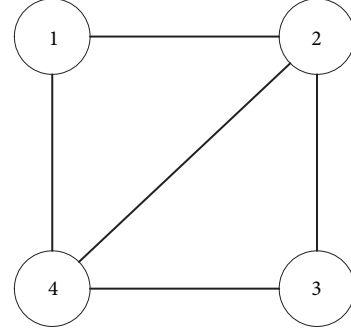


FIGURE 1: The undirected network topology.

$$= \arctan R_l(\omega),$$

$$\Gamma_l(\omega) = \frac{1}{\omega} [\Theta_l(\omega) - \arg(\lambda_i)], \quad (51)$$

where $l \in \{1, 2, 3, 4, 5, 6\}$, $\arg(\lambda_i) \in (-\pi/2, \pi/2)$, λ_i is the i -th eigenvalue of L , $R_l(\omega) \triangleq \text{Im}[B_l(\omega)]/\text{Re}[B_l(\omega)] = \tan[\Theta_l(\omega)]$, and $\text{Im}[B_l(\omega)]$ and $\text{Re}[B_l(\omega)]$ denote the imaginary part and real part of $B_l(\omega)$, respectively.

For the high-order MAS with asymmetric time-delays, if all τ_m satisfy $\tau_m < \bar{\tau} = \min_{|\lambda_i| \neq 0} \{\Gamma_l(\bar{\omega}_i)\}$, then the control protocol (7) can resolve the consensus problem for the high-order MAS with asymmetric time-delays, and on the contrary, then the control protocol (7) can not resolve the consensus problem for the high-order MAS with asymmetric time-delays. The value of $\bar{\omega}_i$ corresponding to l in $\Gamma_l(\bar{\omega}_i)$ is determined by the following equation:

$$|B_l(\bar{\omega}_i)| = |\lambda_i|, \quad l \in \{1, 2, 3, 4, 5, 6\}, \quad (52)$$

where $|B_l(\bar{\omega}_i)|$ is the modulus of $B_l(\bar{\omega}_i)$.

6. Simulation Results

The correctness and validity of the theoretical results for Theorems 4 and 9 will be verified by some numerical simulations in this section. Under different network topologies, the FOMAS with different multiple integral will be considered.

First of all, to validate Theorem 4, we consider a FOMAS composed of 4 agents. Figure 1 shows the network topology depicted with a connected and undirected graph \mathcal{G} , and Figure 1 has five different time-delays which are symmetric time-delays and it shows full connectivity. All the delays are marked with τ_{ij} , where i and j are the indexes, which are used to represent the connected agents i and j . If we suppose the weight of each edge of graph \mathcal{G} in Figure 1 is 1, then the adjacency matrix and

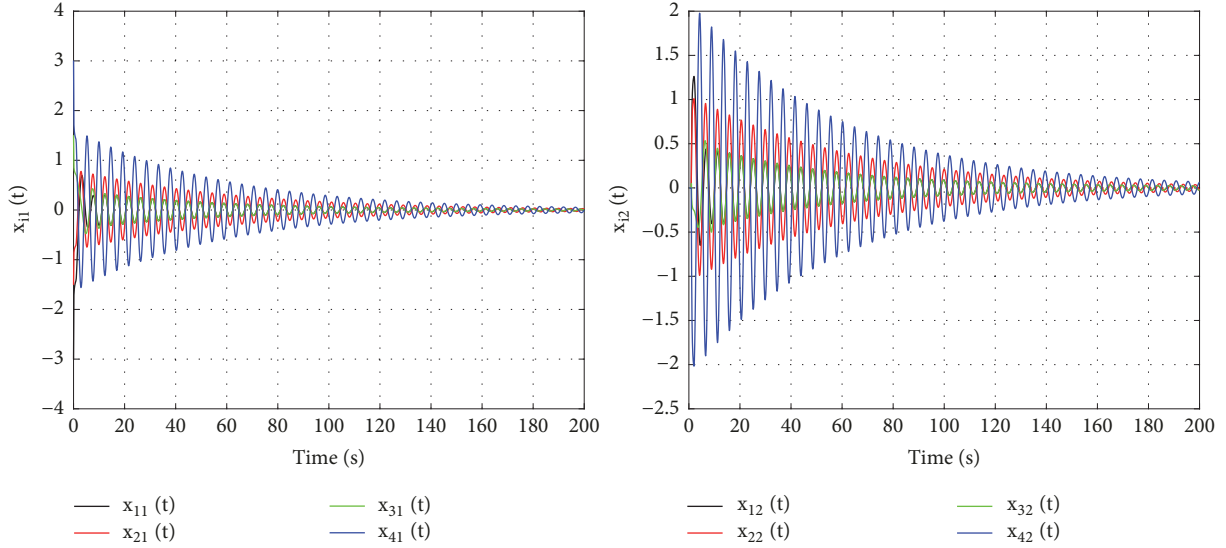


FIGURE 2: The trajectories of all agents' states in the FOMAS with double integral and symmetric time-delays when all $\tau_m < \bar{\tau}$ in Example 1.

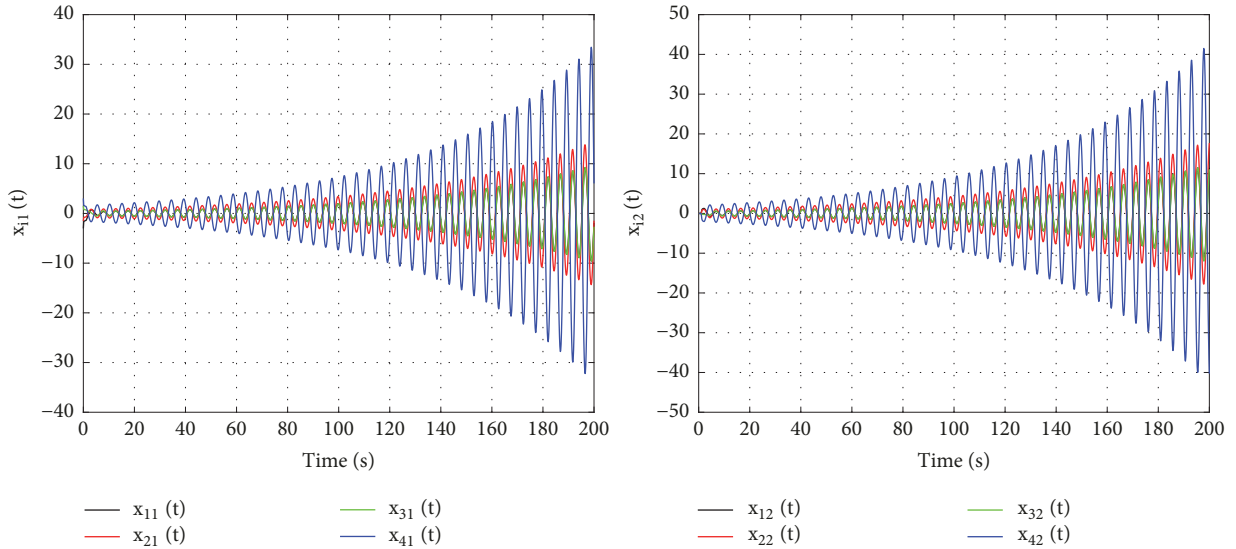


FIGURE 3: The trajectories of all agents' states in the FOMAS with double integral and symmetric time-delays when all $\tau_m > \bar{\tau}$ in Example 1.

the corresponding Laplacian matrix of \mathcal{G} are, respectively,

$$\mathcal{A} = \begin{bmatrix} 2 & 1 & 0 & 1 \\ 1 & 3 & 1 & 1 \\ 0 & 1 & 2 & 1 \\ 1 & 1 & 1 & 3 \end{bmatrix}, \quad (53)$$

$$L = \begin{bmatrix} 2 & -1 & 0 & -1 \\ -1 & 3 & -1 & -1 \\ 0 & -1 & 2 & -1 \\ -1 & -1 & -1 & 3 \end{bmatrix},$$

where $\lambda_n = 4$ is the maximum eigenvalue of L .

Example 1. For a FOMAS with double integral and symmetric time-delays under the undirected graph, let us set $\alpha_1 = 0.9$, $\alpha_2 = 0.8$, $\alpha_l = 0$ ($3 \leq l \leq 6$), and $P_2 = 2.5$, $P_3 = 1$, $P_4 = P_5 = P_6 = P_7 = 0$; thus the delay margin $\bar{\tau} = 1.015s$ according to Theorem 4. Two groups of symmetric time-delays are set: $\tau_{12} = \tau_{21} = 1.01s$, $\tau_{14} = \tau_{41} = 1.00s$, $\tau_{23} = \tau_{32} = 0.99s$, $\tau_{24} = \tau_{42} = 0.98s$, $\tau_{34} = \tau_{43} = 0.97s$, which are bounded by the delay margin $\bar{\tau}$; $\tau_{12} = \tau_{21} = 1.02s$, $\tau_{14} = \tau_{41} = 1.03s$, $\tau_{23} = \tau_{32} = 1.04s$, $\tau_{24} = \tau_{42} = 1.05s$, $\tau_{34} = \tau_{43} = 1.06s$, which exceed the delay margin $\bar{\tau}$. The simulation results about Example 1 are displayed in Figures 2 and 3: the two subfigures in Figure 2 show the trajectories of all agents' states when all symmetric time-delays are less than the delay margin $\bar{\tau}$, which indicates that the FOMAS with double integral and symmetric time-delays is stable and consensus

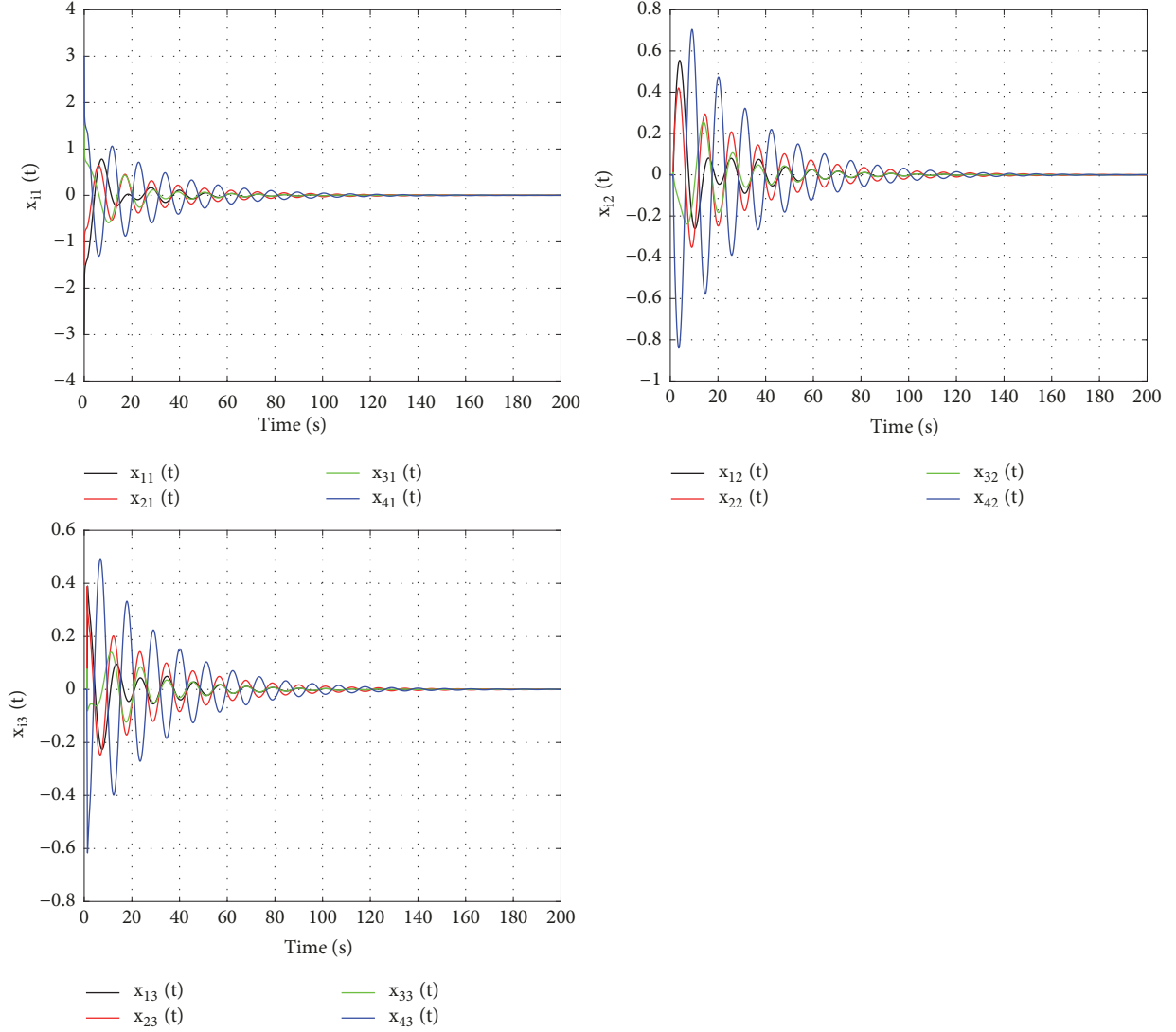


FIGURE 4: The trajectories of all agents' states in the FOMAS with triple integral and symmetric time-delays when all $\tau_m < \bar{\tau}$ in Example 2.

of the FOMAS with double integral and symmetric time-delays can be reached; the two subfigures in Figure 3 show the trajectories of all agents' states when all symmetric time-delays exceed the delay margin $\bar{\tau}$, which indicates that the FOMAS with double integral and symmetric time-delays is unstable and consensus of the FOMAS with double integral and symmetric time-delays can not be reached.

Example 2. For a FOMAS with triple integral and symmetric time-delays under the undirected graph, let us set $\alpha_1 = 0.9$, $\alpha_2 = 0.8$, $\alpha_3 = 0.7$, $\alpha_l = 0$ ($4 \leq l \leq 6$), and $P_2 = 2.5$, $P_3 = 9$, $P_4 = 1$, $P_5 = P_6 = P_7 = 0$; thus $\bar{\tau} = 1.398s$ according to Theorem 4. Two groups of symmetric time-delays are set: $\tau_{12} = \tau_{21} = 1.30s$, $\tau_{14} = \tau_{41} = 1.25s$, $\tau_{23} = \tau_{32} = 1.20s$, $\tau_{24} = \tau_{42} = 1.15s$, $\tau_{34} = \tau_{43} = 1.10s$, which are bounded by the delay margin $\bar{\tau}$; $\tau_{12} = \tau_{21} = 1.40s$, $\tau_{14} = \tau_{41} = 1.41s$, $\tau_{23} = \tau_{32} = 1.42s$, $\tau_{24} = \tau_{42} = 1.43s$,

$\tau_{34} = \tau_{43} = 1.44s$, which exceed the delay margin $\bar{\tau}$. The simulation results about Example 2 are displayed in Figures 4 and 5: the three subfigures in Figure 4 show the trajectories of all agents' states when all symmetric time-delays are less than the delay margin $\bar{\tau}$, which indicates that the FOMAS with triple integral and symmetric time-delays is stable and consensus of the FOMAS with triple integral and symmetric time-delays can be reached; the three subfigures in Figure 5 show the trajectories of all agents' states when all symmetric time-delays exceed the delay margin $\bar{\tau}$, which indicates that the FOMAS with triple integral and symmetric time-delays is unstable and consensus of the FOMAS with triple integral and symmetric time-delays can not be reached.

Example 3. For a FOMAS with sextuple integral and symmetric time-delays under the undirected graph, let us set $\alpha_1 = 0.9$, $\alpha_2 = 0.8$, $\alpha_3 = 0.7$, $\alpha_4 = 0.6$, $\alpha_5 = 0.5$, $\alpha_6 = 0.4$, and

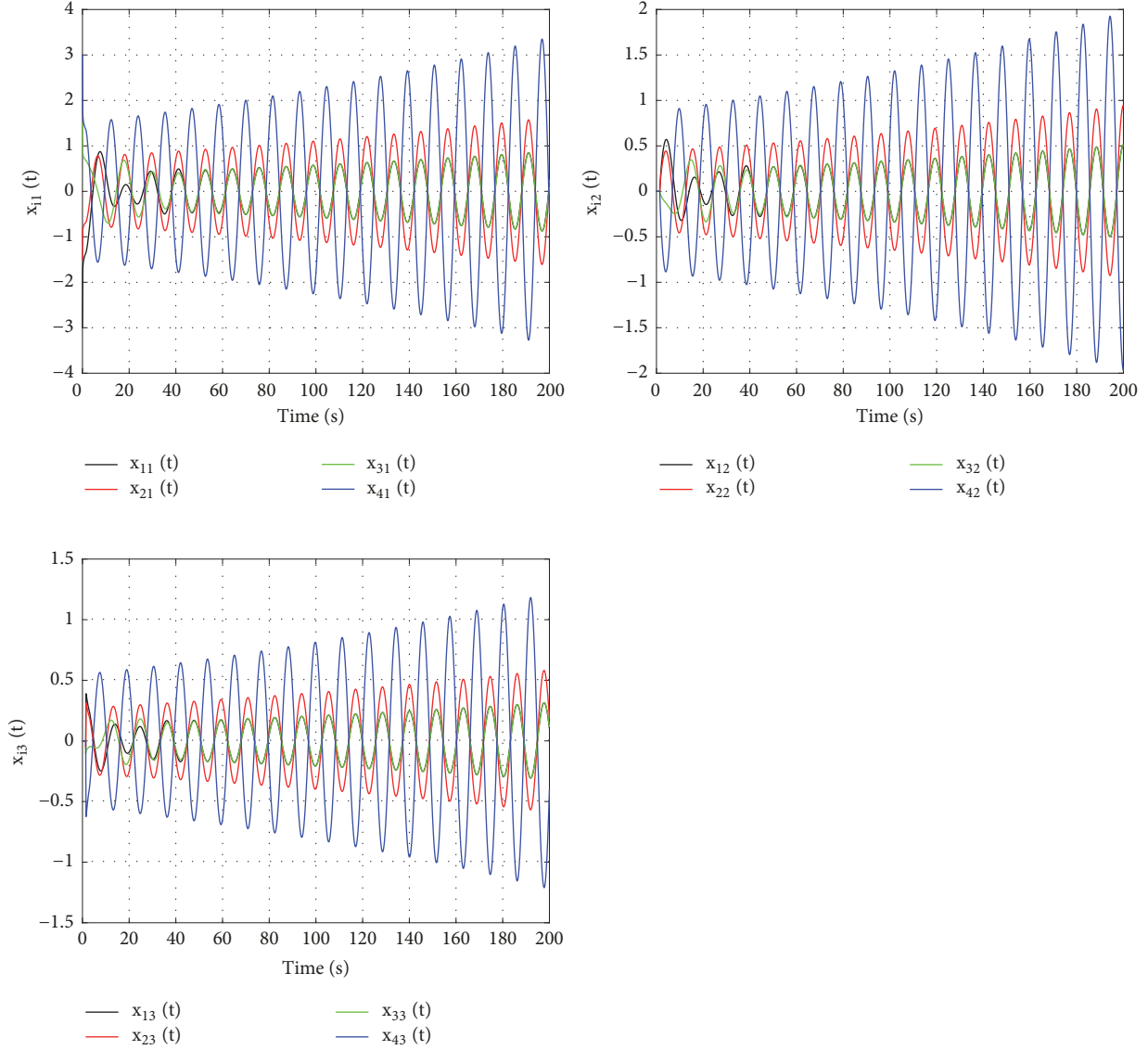


FIGURE 5: The trajectories of all agents' states in the FOMAS with triple integral and symmetric time-delays when all $\tau_m > \bar{\tau}$ in Example 2.

$P_2 = 2.5$, $P_3 = 9$, $P_4 = 4$, $P_5 = 8$, $P_6 = 1.2$, $P_7 = 1$; thus $\bar{\tau} = 0.2515s$ according to Theorem 4. Two groups of symmetric time-delays are set: $\tau_{12} = \tau_{21} = 0.24s$, $\tau_{14} = \tau_{41} = 0.22s$, $\tau_{23} = \tau_{32} = 0.20s$, $\tau_{24} = \tau_{42} = 0.18s$, $\tau_{34} = \tau_{43} = 0.16s$, which are bounded by the delay margin $\bar{\tau}$; $\tau_{12} = \tau_{21} = 0.26s$, $\tau_{14} = \tau_{41} = 0.27s$, $\tau_{23} = \tau_{32} = 0.28s$, $\tau_{24} = \tau_{42} = 0.29s$, $\tau_{34} = \tau_{43} = 0.30s$, which exceed the delay margin $\bar{\tau}$. The simulation results about Example 3 are displayed in Figures 6 and 7: the six subfigures in Figure 6 show the trajectories of all agents' states when all symmetric time-delays are less than the delay margin $\bar{\tau}$, which indicates that the FOMAS with sextuple integral and symmetric time-delays is stable and consensus of the FOMAS with sextuple integral and symmetric time-delays can be reached; the six subfigures in Figure 7 show the trajectories of all agents' states when all symmetric time-delays exceed the delay margin $\bar{\tau}$, which indicates that the

FOMAS with sextuple integral and symmetric time-delays is unstable and consensus of the FOMAS with sextuple integral and symmetric time-delays can not be reached.

Next, to examine Theorem 9, we give a network topology described in Figure 8, which is a directed graph \mathcal{G} with a spanning tree. It also contains five different time-delays which are asymmetric time-delays and displays full connectivity. If we suppose the weight of each edge of graph \mathcal{G} in Figure 8 is 1, then the adjacency matrix and the corresponding Laplacian matrix are

$$\mathcal{A} = \begin{bmatrix} 2 & 1 & 0 & 1 \\ 0 & 1 & 0 & 1 \\ 0 & 1 & 1 & 0 \\ 0 & 0 & 1 & 1 \end{bmatrix},$$

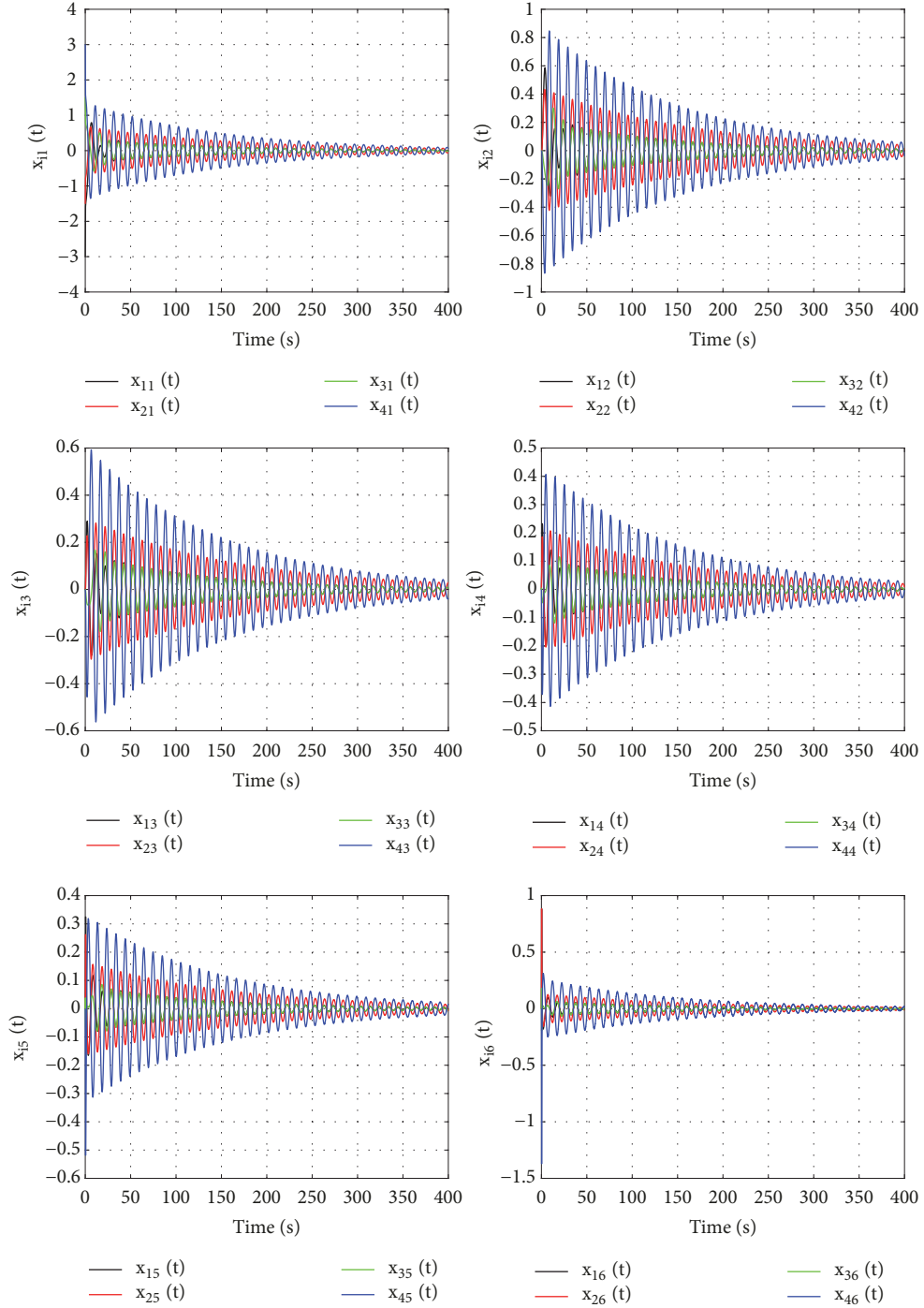


FIGURE 6: The trajectories of all agents' states in the FOMAS with sextuple integral and symmetric time-delays when all $\tau_m < \bar{\tau}$ in Example 3.

$$L = \begin{bmatrix} 2 & -1 & 0 & -1 \\ 0 & 1 & 0 & -1 \\ 0 & -1 & 1 & 0 \\ 0 & 0 & -1 & 1 \end{bmatrix},$$

(54)

where $\lambda_1 = 2, \lambda_2 = 0, \lambda_3 = 1.5 + 0.866i$, and $\lambda_4 = 1.5 - 0.866i$ are all eigenvalues of L .

Example 4. For a FOMAS with double integral and asymmetric time-delays under the directed graph, let us set $\alpha_1 = 0.9, \alpha_2 = 0.8, \alpha_l = 0$ ($3 \leq l \leq 6$), and $P_2 = 2.5, P_3 = 1, P_4 = P_5 = P_6 = P_7 = 0$; thus $\bar{\tau} = 1.649s$ according to

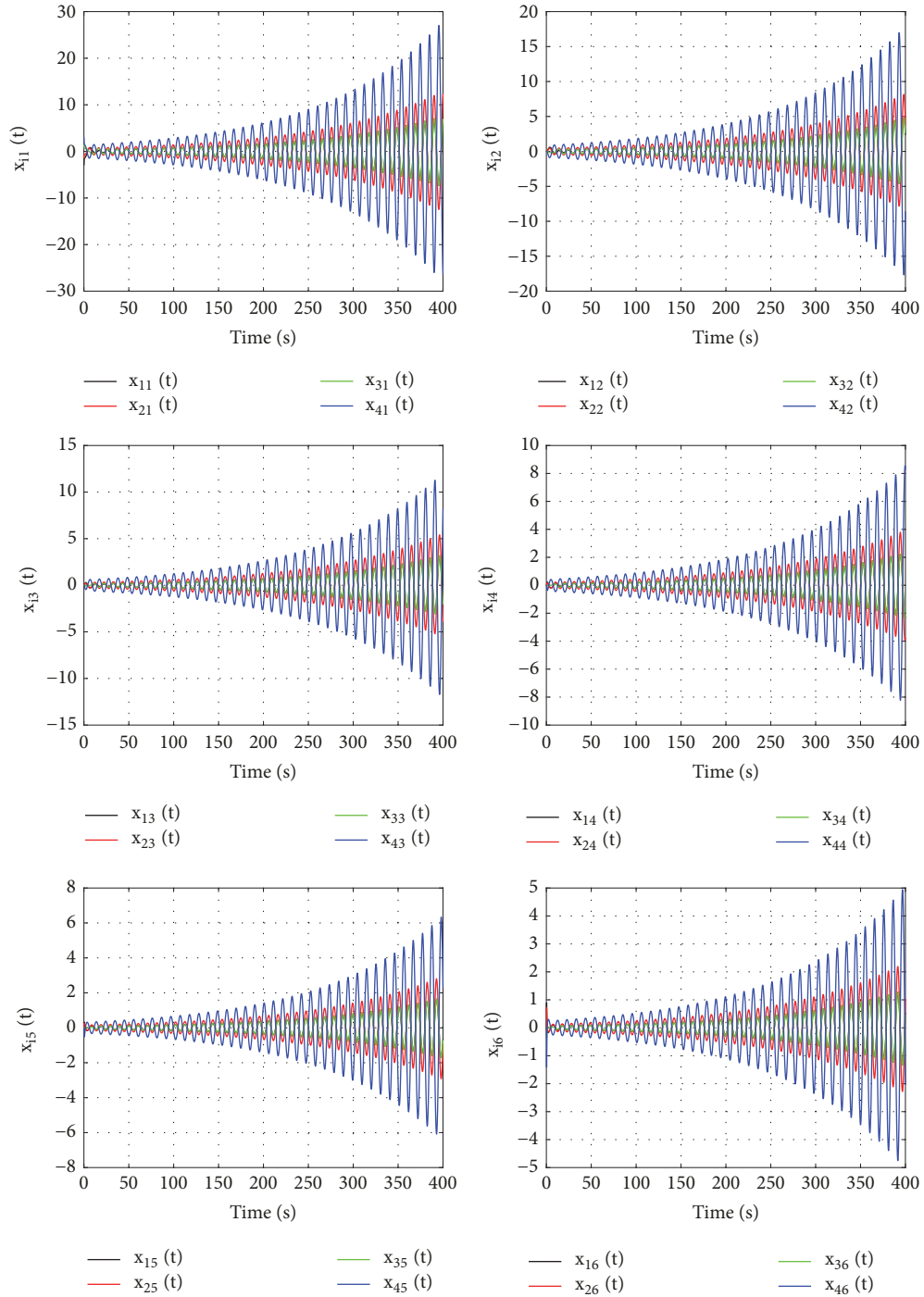


FIGURE 7: The trajectories of all agents' states in the FOMAS with sextuple integral and symmetric time-delays when all $\tau_m > \bar{\tau}$ in Example 3.

Theorem 9. Two groups of asymmetric time-delays are set: $\tau_{12} = 1.64s$, $\tau_{14} = 1.63s$, $\tau_{24} = 1.62s$, $\tau_{32} = 1.61s$, $\tau_{43} = 1.60s$, which are bounded by the delay margin $\bar{\tau}$; $\tau_{12} = 1.66s$, $\tau_{14} = 1.67s$, $\tau_{24} = 1.68s$, $\tau_{32} = 1.69s$, $\tau_{43} = 1.70s$, which exceed the delay margin $\bar{\tau}$. The simulation results about Example 4 are displayed in Figures 9 and 10: the two

subfigures in Figure 9 show the trajectories of all agents' states when all asymmetric time-delays are less than the delay margin $\bar{\tau}$, which indicates that consensus of the FOMAS with double integral and asymmetric time-delays can be reached; the two subfigures in Figure 10 show the trajectories of all agents' states when all asymmetric time-delays exceed the

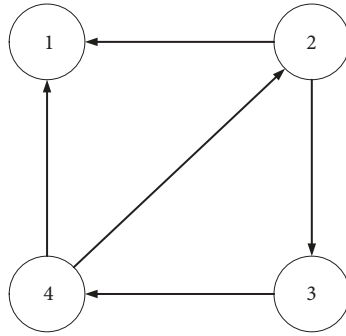


FIGURE 8: The directed network topology.

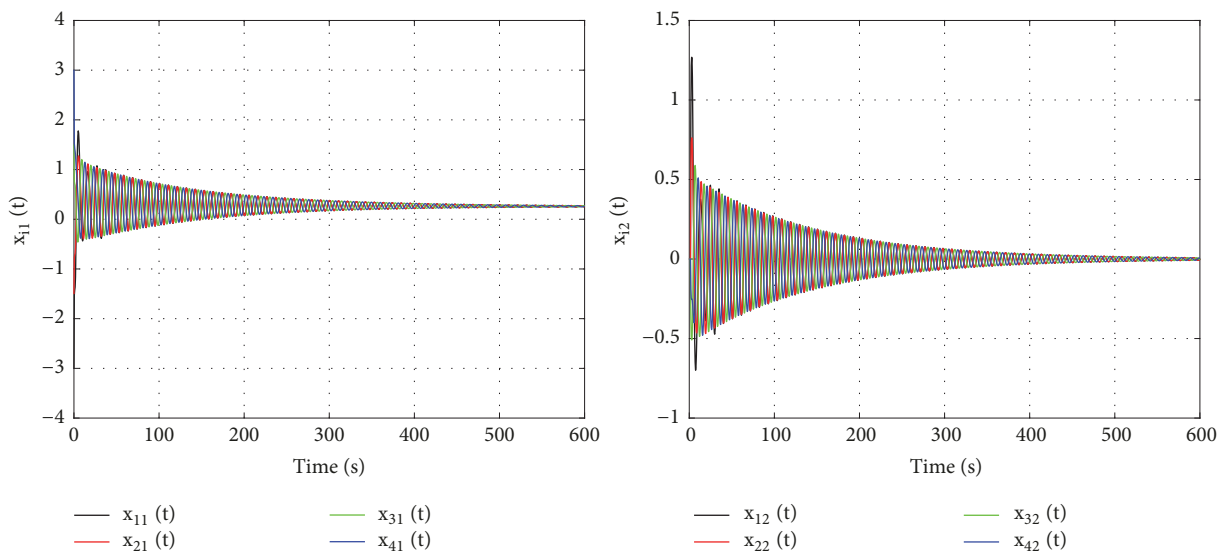


FIGURE 9: The trajectories of all agents' states in the FOMAS with double integral and asymmetric time-delays when all $\tau_m < \bar{\tau}$ in Example 4.

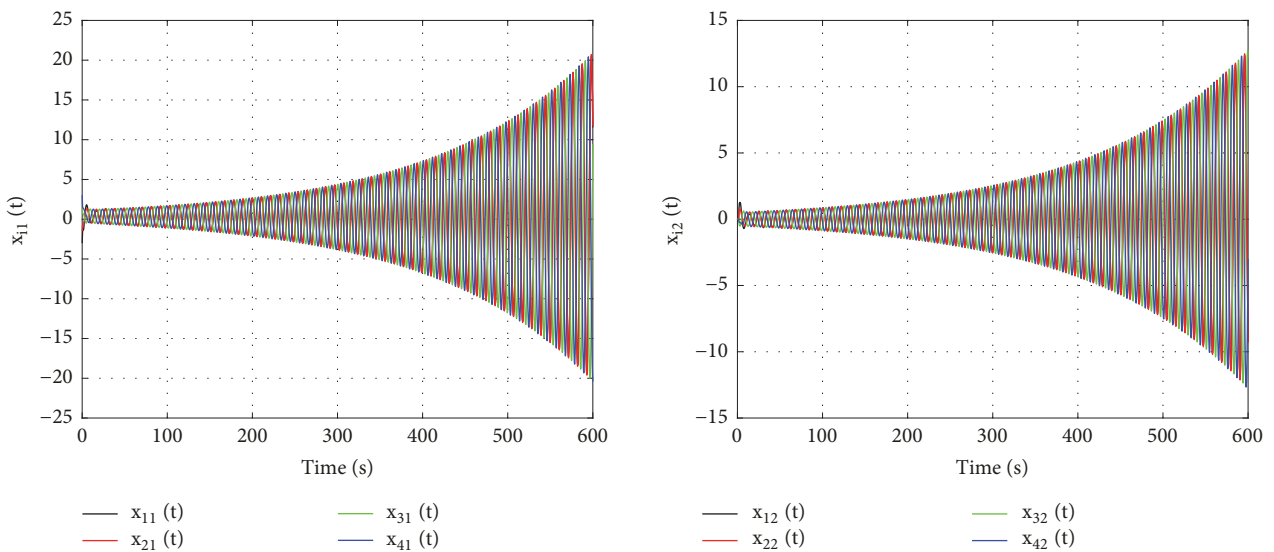


FIGURE 10: The trajectories of all agents' states in the FOMAS with double integral and asymmetric time-delays when all $\tau_m > \bar{\tau}$ in Example 4.

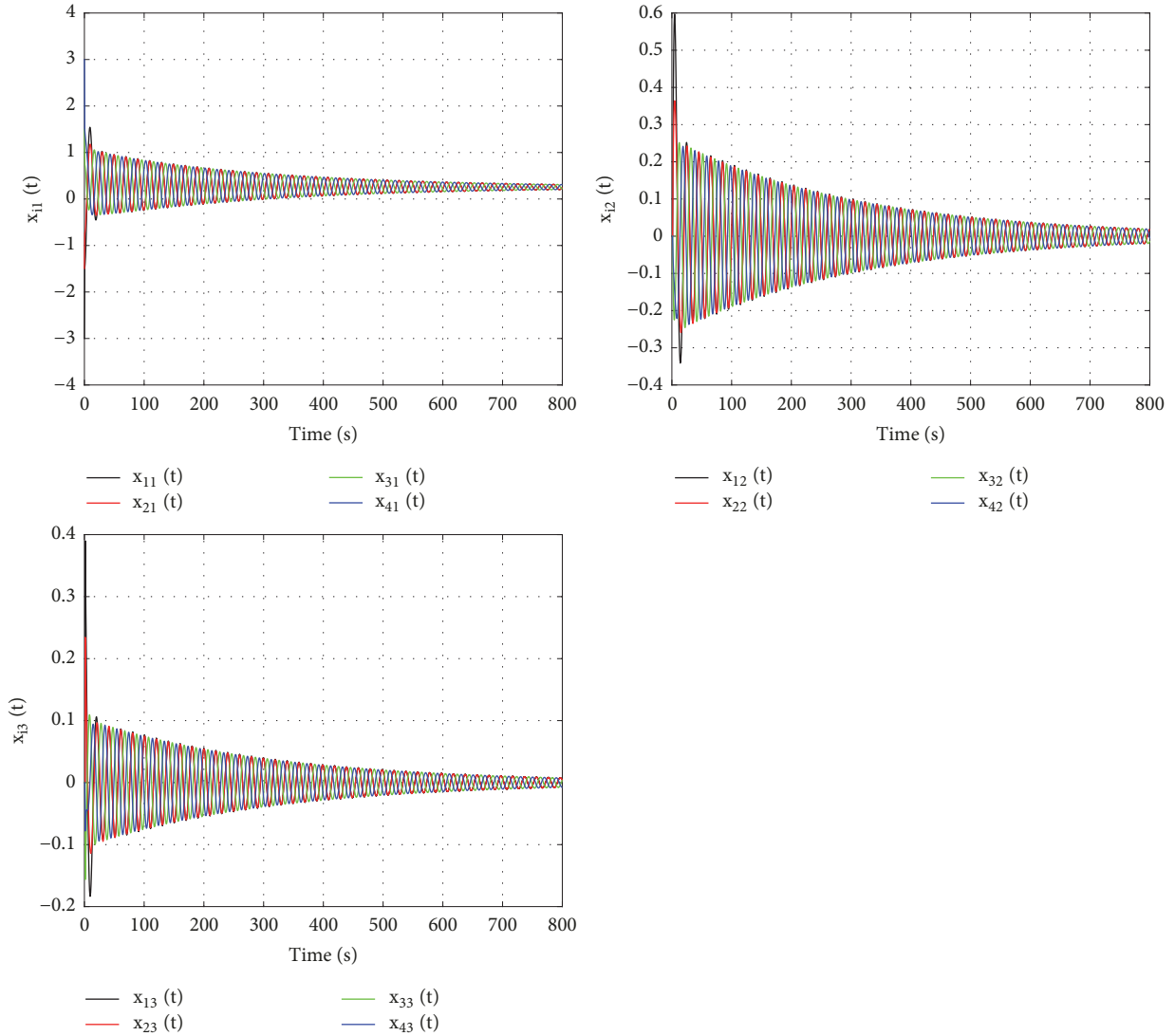


FIGURE 11: The trajectories of all agents' states in the FOMAS with triple integral and asymmetric time-delays when all $\tau_m < \bar{\tau}$ in Example 5.

delay margin $\bar{\tau}$, which indicates that consensus of the FOMAS with double integral and asymmetric time-delays can not be reached.

Example 5. For a FOMAS with triple integral and asymmetric time-delays under the directed graph, let us set $\alpha_1 = 0.9$, $\alpha_2 = 0.8$, $\alpha_3 = 0.7$, $\alpha_l = 0$ ($4 \leq l \leq 6$), and $P_2 = 2.5$, $P_3 = 9$, $P_4 = 1$, $P_5 = P_6 = P_7 = 0$; thus $\bar{\tau} = 1.327s$ according to Theorem 9. Two groups of asymmetric time-delays are set: $\tau_{12} = 1.32s$, $\tau_{14} = 1.29s$, $\tau_{24} = 1.26s$, $\tau_{32} = 1.23s$, $\tau_{43} = 1.21s$, which are bounded by the delay margin $\bar{\tau}$; $\tau_{12} = 1.33s$, $\tau_{14} = 1.36s$, $\tau_{24} = 1.39s$, $\tau_{32} = 1.42s$, $\tau_{43} = 1.45s$, which exceed the delay margin $\bar{\tau}$. The simulation results about Example 5 are displayed in Figures 11 and 12: the three subfigures in Figure 11 show the trajectories of all agents' states when all asymmetric time-delays are less than the delay margin $\bar{\tau}$, which indicates that consensus of the FOMAS with

triple integral and asymmetric time-delays can be reached; the three subfigures in Figure 12 show the trajectories of all agents' states when all asymmetric time-delays exceed the delay margin $\bar{\tau}$, which indicates that consensus of the FOMAS with triple integral and asymmetric time-delays can not be reached.

Example 6. For a FOMAS with sextuple integral and asymmetric time-delays under the directed graph, let us set $\alpha_1 = 0.9$, $\alpha_2 = 0.8$, $\alpha_3 = 0.7$, $\alpha_4 = 0.6$, $\alpha_5 = 0.5$, $\alpha_6 = 0.4$, and $P_2 = 2.5$, $P_3 = 9$, $P_4 = 4$, $P_5 = 8$, $P_6 = 1.2$, $P_7 = 1$; thus $\bar{\tau} = 0.4335s$ according to Theorem 9. Two groups of asymmetric time-delays are set: $\tau_{12} = 0.43s$, $\tau_{14} = 0.40s$, $\tau_{24} = 0.37s$, $\tau_{32} = 0.34s$, $\tau_{43} = 0.31s$, which are bounded by the delay margin $\bar{\tau}$; $\tau_{12} = 0.44s$, $\tau_{14} = 0.47s$, $\tau_{24} = 0.50s$, $\tau_{32} = 0.53s$, $\tau_{43} = 0.57s$, which exceed the delay margin $\bar{\tau}$. The simulation results about Example 6 are

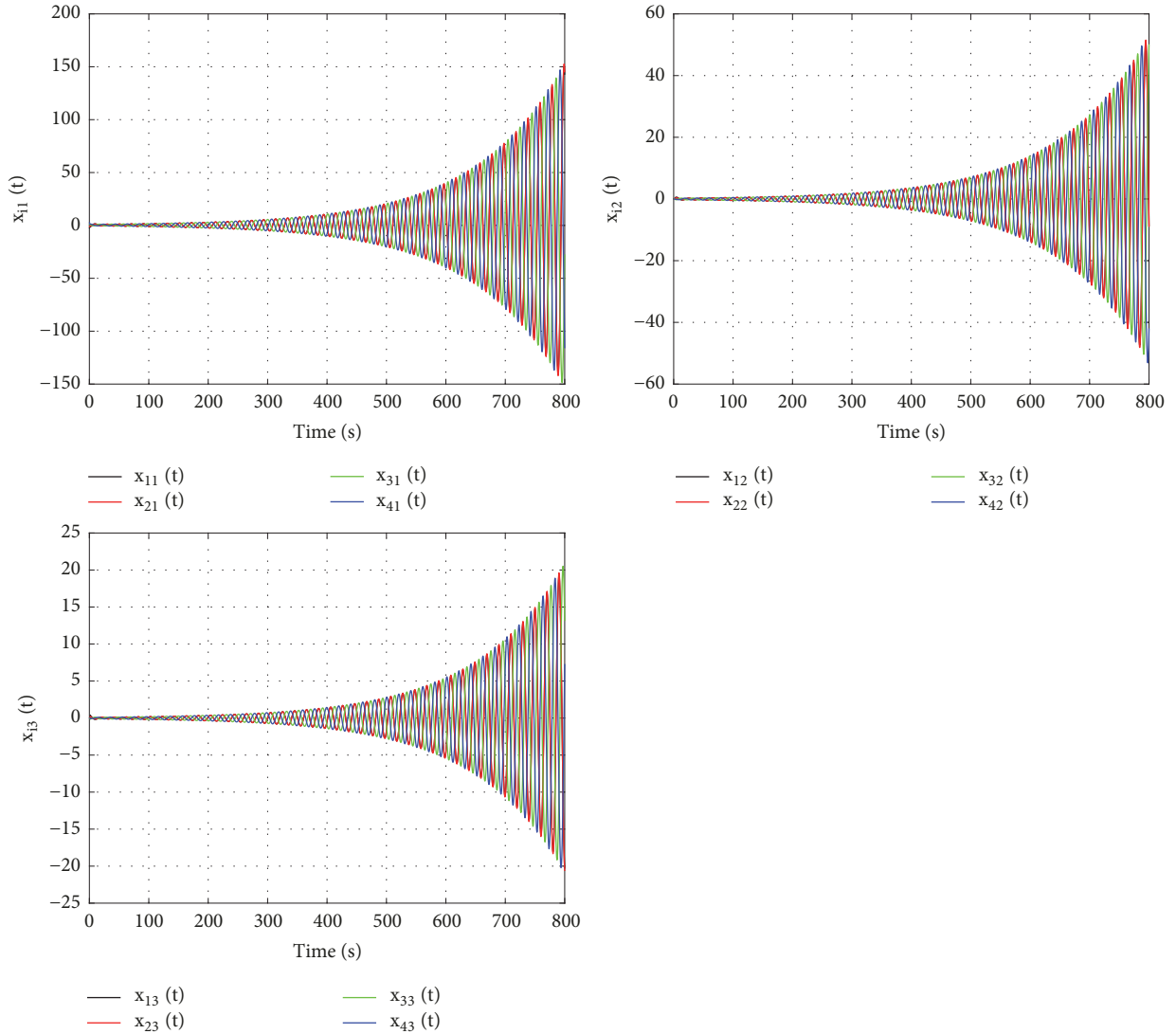


FIGURE 12: The trajectories of all agents' states in the FOMAS with triple integral and asymmetric time-delays when all $\tau_m > \bar{\tau}$ in Example 5.

displayed in Figures 13 and 14: the six subfigures in Figure 13 show the trajectories of all agents' states when all asymmetric time-delays are less than the delay margin $\bar{\tau}$, which indicates that consensus of the FOMAS with sextuple integral and asymmetric time-delays can be reached; the six subfigures in Figure 14 show the trajectories of all agents' states when all asymmetric time-delays exceed the delay margin $\bar{\tau}$, which indicates that consensus of the FOMAS with sextuple integral and asymmetric time-delays can not be reached.

7. Conclusion

The consensus problems of a FOMAS with multiple integral under nonuniform time-delays are studied in this paper. Taking into account two kinds of nonuniform time-delays, the sufficient conditions have been derived in the form of inequalities for the MIFOMAS with nonuniform time-delays. Numerical simulations of the MIFOMAS with nonuniform

time-delays over undirected topology and directed topology are performed to verify these theorems. Finally, the simulation results show that the selected examples have achieved the desired results: the MIFOMAS with nonuniform time-delays under given conditions can achieve the consensus. With the help of the above research of this paper, distributed formation control of the MIFOMAS with nonuniform time-delays will be one of the most significant topics, which will be one of our future research tasks.

Data Availability

The data used to support the findings of this study are available from the corresponding author upon request.

Conflicts of Interest

The authors declare that they have no conflicts of interest.

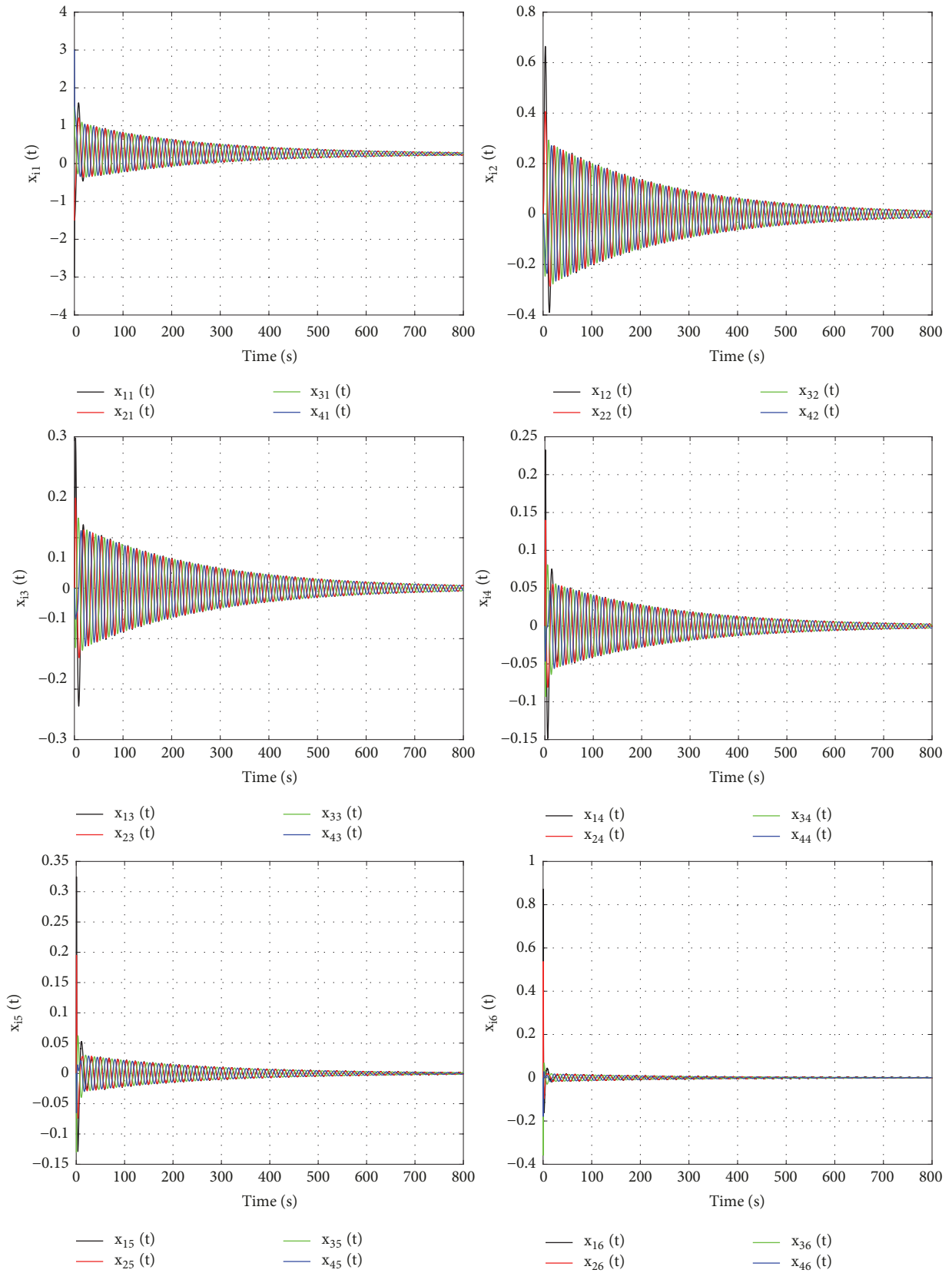


FIGURE 13: The trajectories of all agents' states in the FOMAS with sextuple integral and asymmetric time-delays when all $\tau_m < \bar{\tau}$ in Example 6.

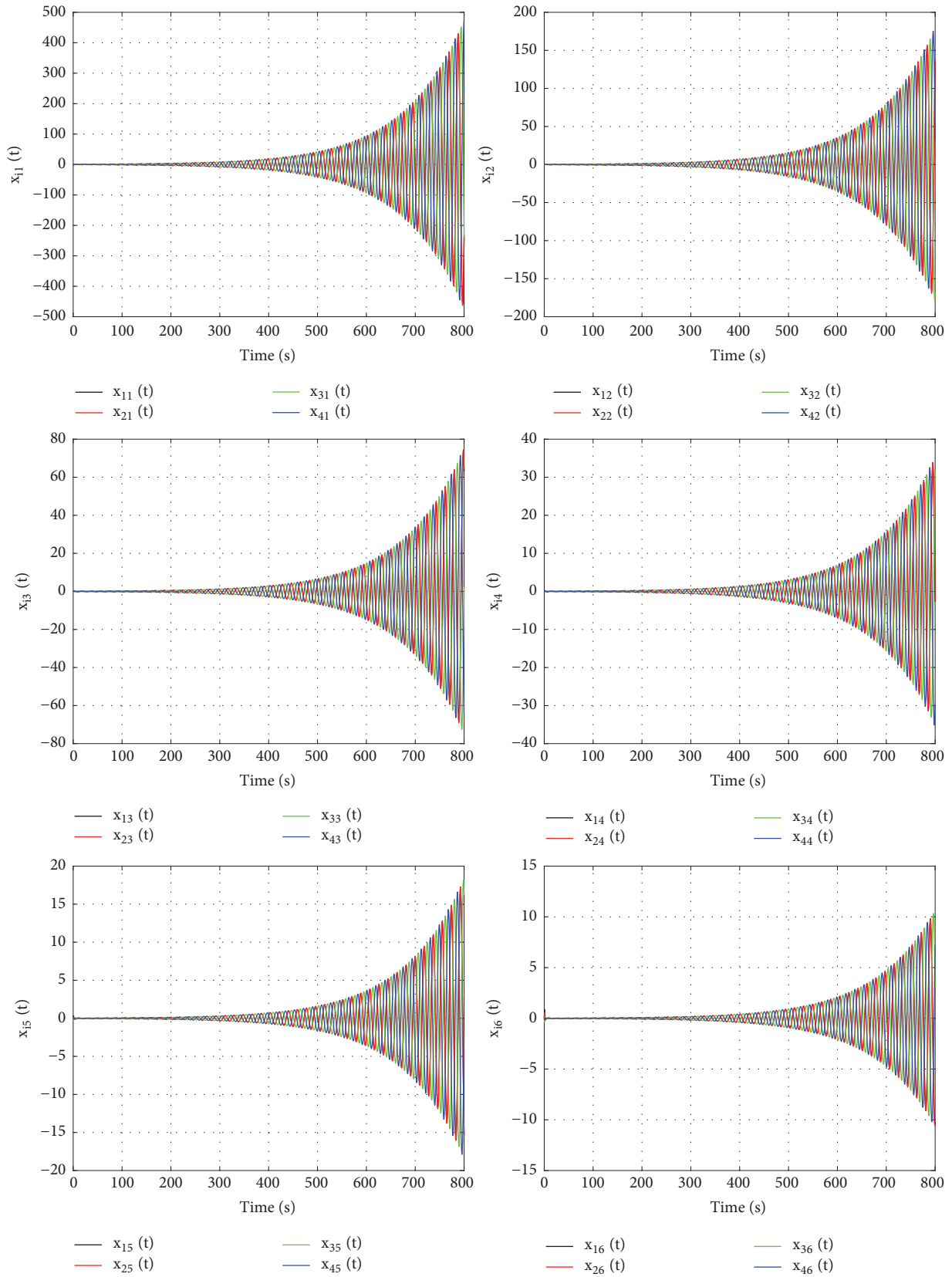


FIGURE 14: The trajectories of all agents' states in the FOMAS with sextuple integral and asymmetric time-delays when all $\tau_m > \bar{\tau}$ in Example 6.

Acknowledgments

This work was supported by the Science and Technology Department Project of Sichuan Province of China (Grants nos. 2014FZ0041, 2017GZ0305, and 2016GZ0220), the Education Department Key Project of Sichuan Province of China (Grant no. 17ZA0077), and the National Natural Science Foundation of China (Grant nos. U1733103, 61802036).

References

- [1] M. Shi, K. Qin, and J. Liu, "Cooperative multi-agent sweep coverage control for unknown areas of irregular shape," *Iet Control Theory and Applications*, vol. 18, no. 2, pp. 115–117, 2008.
- [2] A. E. Turgut, H. Çelikkıran, F. Gökçe, and E. Şahin, "Self-organized flocking in mobile robot swarms," *Swarm Intelligence*, vol. 2, no. 2-4, pp. 97–120, 2008.
- [3] T. R. Krogstad and J. T. Gravdahl, *Coordinated Attitude Control of Satellites in Formation*, Springer Berlin Heidelberg, 2006.
- [4] T. Vicsek, A. Czirak, E. Ben-Jacob, I. Cohen, and O. Shochet, "Novel type of phase transition in a system of self-driven particles," *Physical Review Letters*, vol. 75, no. 6, pp. 1226–1229, 1995.
- [5] A. Jadbabaie, J. Lin, and A. S. Morse, "Coordination of groups of mobile autonomous agents using nearest neighbor rules," *IEEE Transactions on Automatic Control*, vol. 48, no. 6, pp. 988–1001, 2003.
- [6] L. Moreau, "Stability of multiagent systems with time-dependent communication links," *IEEE Transactions on Automatic Control*, vol. 50, no. 2, pp. 169–182, 2005.
- [7] W. Ren and R. W. Beard, "Consensus seeking in multiagent systems under dynamically changing interaction topologies," *IEEE Transactions on Automatic Control*, vol. 50, no. 5, pp. 655–661, 2005.
- [8] R. Olfati-Saber, J. A. Fax, and R. M. Murray, "Consensus and cooperation in networked multi-agent systems," *Proceedings of the IEEE*, vol. 95, no. 1, pp. 215–233, 2007.
- [9] P. Li and K. Qin, "Distributed robust h_{∞} consensus control for uncertain multiagent systems with state and input delays," *Mathematical Problems in Engineering*, vol. 2017, Article ID 5091756, 15 pages, 2017.
- [10] Y. Wu, B. Hu, and Z. Guan, "Exponential Consensus Analysis for Multiagent Networks Based on Time-Delay Impulsive Systems," *IEEE Transactions on Systems, Man, and Cybernetics: Systems*, vol. 99, pp. 1–8, 2017.
- [11] Y. Wu, B. Hu, and Z. Guan, "Consensus Problems Over Cooperation-Competition Random Switching Networks With Noisy Channels," *IEEE Transactions on Neural Networks and Learning Systems*, vol. 99, pp. 1–9, 2018.
- [12] P. Lin and Y. Jia, "Consensus of a class of second-order multi-agent systems with time-delay and jointly-connected topologies," *IEEE Transactions on Automatic Control*, vol. 55, no. 3, pp. 778–784, 2010.
- [13] J. Qin, H. Gao, and W. X. Zheng, "Second-order consensus for multi-agent systems with switching topology and communication delay," *Systems & Control Letters*, vol. 60, no. 6, pp. 390–397, 2011.
- [14] H. Li, X. Liao, X. Lei, T. Huang, and W. Zhu, "Second-order consensus seeking in multi-agent systems with nonlinear dynamics over random switching directed networks," *IEEE Transactions on Circuits and Systems I: Regular Papers*, vol. 60, no. 6, pp. 1595–1607, 2013.
- [15] P. Li, K. Qin, and M. Shi, "Distributed robust H_{∞} rotating consensus control for directed networks of second-order agents with mixed uncertainties and time-delay," *Neurocomputing*, vol. 148, pp. 332–339, 2015.
- [16] M. Shi and K. Qin, "Distributed Control for Multiagent Consensus Motions with Nonuniform Time Delays," *Mathematical Problems in Engineering*, vol. 2016, Article ID 3567682, 10 pages, 2016.
- [17] Y. Liu and Y. M. Jia, "Consensus problem of high-order multi-agent systems with external disturbances: an h_8 analysis approach," *International Journal of Robust & Nonlinear Control*, vol. 20, no. 14, pp. 1579–1593, 2010.
- [18] P. Lin, Z. Li, Y. Jia, and M. Sun, "High-order multi-agent consensus with dynamically changing topologies and time-delays," *IET Control Theory & Applications*, vol. 5, no. 8, pp. 976–981, 2011.
- [19] Y.-P. Tian and Y. Zhang, "High-order consensus of heterogeneous multi-agent systems with unknown communication delays," *Automatica*, vol. 48, no. 6, pp. 1205–1212, 2012.
- [20] J. Liu and B. Zhang, "Consensus Problem of High-Order Multiagent Systems with Time Delays," *Mathematical Problems in Engineering*, vol. 2017, Article ID 9104905, 7 pages, 2017.
- [21] M. Shi, K. Qin, P. Li, and J. Liu, "Consensus Conditions for High-Order Multiagent Systems with Nonuniform Delays," *Mathematical Problems in Engineering*, vol. 2017, Article ID 7307834, 12 pages, 2017.
- [22] W. Ren and Y. C. Cao, *Distributed Coordination of Multi-agent Networks*, Springer, London, UK, 2011.
- [23] R. C. Koeller, "Toward an equation of state for solid materials with memory by use of the half-order derivative," *Acta Mechanica*, vol. 191, no. 3-4, pp. 125–133, 2007.
- [24] J. Sabatier, O. P. Agrawal, and J. A. Machado, "Advance in Fractional Calculus: Theoretical Developments and Applications in Physics and Engineering," *Biochemical Journal*, vol. 361, no. 1, pp. 97–103, 2007.
- [25] J. Bai, G. Wen, A. Rahmani, X. Chu, and Y. Yu, "Consensus with a reference state for fractional-order multi-agent systems," *International Journal of Systems Science*, vol. 47, no. 1, pp. 222–234, 2016.
- [26] G. Ren and Y. Yu, "Consensus of fractional multi-agent systems using distributed adaptive protocols," *Asian Journal of Control*, vol. 19, no. 6, pp. 2076–2084, 2017.
- [27] C. Tricaud and Y. Chen, "Time-Optimal Control of Systems with Fractional Dynamics," *International Journal of Differential Equations*, vol. 2010, Article ID 461048, 16 pages, 2010.
- [28] Z. Liao, C. Peng, W. Li, and Y. Wang, "Robust stability analysis for a class of fractional order systems with uncertain parameters," *Journal of The Franklin Institute*, vol. 348, no. 6, pp. 1101–1113, 2011.
- [29] Y. C. Cao, Y. Li, W. Ren, and Y. Q. Chen, "Distributed coordination of networked fractional-order systems," *IEEE Transactions on Systems, Man, and Cybernetics, Part B: Cybernetics*, vol. 40, no. 2, pp. 362–370, 2010.
- [30] H. Y. Yang, X. L. Zhu, and K. C. Cao, "Distributed coordination of fractional order multi-agent systems with communication delays," *Fractional Calculus Applied Analysis*, vol. 17, no. 1, pp. 23–37, 2013.

- [31] H. Y. Yang, L. Guo, X. L. Zhu, K. C. Cao, and H. L. Zou, "Consensus of compound-order multi-agent systems with communication delays," *Central European Journal of Physics*, vol. 11, no. 6, pp. 806–812, 2013.
- [32] W. Zhu, B. Chen, and Y. Jie, "Consensus of fractional-order multi-agent systems with input time delay," *Fractional Calculus and Applied Analysis*, vol. 20, no. 1, pp. 52–70, 2017.
- [33] J. Liu, K. Qin, W. Chen, P. Li, and M. Shi, "Consensus of Fractional-Order Multiagent Systems with Nonuniform Time Delays," *Mathematical Problems in Engineering*, vol. 2018, Article ID 2850757, 9 pages, 2018.
- [34] J. Liu, K. Y. Qin, W. Chen, and P. Li, "Consensus of delayed fractional-order multi-agent systems based on state-derivative feedback," *Complexity*, vol. 2018, Article ID 8789632, 12 pages, 2018.
- [35] C. Yang, W. Li, and W. Zhu, "Consensus analysis of fractional-order multiagent systems with double-integrator," *Discrete Dynamics in Nature and Society*, 8 pages, 2017.
- [36] S. Shen, W. Li, and W. Zhu, "Consensus of fractional-order multiagent systems with double integrator under switching topologies," *Discrete Dynamics in Nature and Society*, 7 pages, 2017.
- [37] J. Bai, G. Wen, A. Rahmani, and Y. Yu, "Consensus for the fractional-order double-integrator multi-agent systems based on the sliding mode estimator," *IET Control Theory & Applications*, vol. 12, no. 5, pp. 621–628, 2018.
- [38] J. Liu, W. Chen, K. Qin, and P. Li, "Consensus of Fractional-Order Multiagent Systems with Double Integral and Time Delay," *Mathematical Problems in Engineering*, vol. 2018, Article ID 6059574, 12 pages, 2018.
- [39] J. Liu, K. Qin, P. Li, and W. Chen, "Distributed consensus control for double-integrator fractional-order multi-agent systems with nonuniform time-delays," *Neurocomputing*, vol. 321, pp. 369–380, 2018.
- [40] I. Podlubny, "Fractional differential equations," *Mathematics in Science & Engineering*, vol. 198, no. 3, pp. 553–556, 1999.
- [41] C. Godsil and G. Royle, *Algebraic Graph Theory*, World Book Publishing Company Beijing Inc, 2014.
- [42] D. Matignon, "Stability properties for generalized fractional differential systems," *Proceedings of the Fractional Differential Systems: Models, Methods and Applications*, vol. 5, pp. 145–158, 1998.

